Research Article

Nano Biomed Eng

Design and Development of Self-nanoemulsifying Drug Delivery System (SNEDDS) with Morin Hydrate to Enhance Nimodipine's oral Bioavailability and Pharmacokinetics

Nirav Patel✉, Priya Patel, Dhara Thummar

Department of Pharmaceutical Sciences, Saurashtra University, Rajkot, India

✉ Corresponding author. E-mail: niarv2564@gmail.com

Received: Sep. 1, 2024; **Revised:** Oct. 14, 2024; **Accepted:** Nov. 10, 2024

Citation: N. Patel, P. Patel, D. Thummar. Design and development of self-nanoemulsifying drug delivery system (snedds) with morin hydrate to enhance nimodipine's oral bioavailability and pharmacokinetics. *Nano Biomedicine and Engineering*, 2024, 16(4): 601−624.

http://doi.org/10.26599/NBE.2024.929016

Abstract

Nimodipine (NMD), a calcium channel blocker, is classified as a Biopharmaceutical Classification System Class II drug, with low oral bioavailability (3%–30%) due to extensive first-pass metabolism. Self-nanoemulsifying drug delivery systems (SNEDDS) offer a novel approach to improving the bioavailability of such drugs. Morin hydrate (MH), a flavonoid, may enhance NMD's bioavailability by modulating CYP3A4 and P-glycoprotein during metabolism. This study aimed to optimize an MH-loaded NMD-SNEDDS formulation using a three-factor, three-level Box–Behnken design (BBD). Independent variables were Capmul MCM (X_1) as the oil, Cremophor RH-40 (X_2) as the surfactant, and Transcutol-P (X_3) as the co-surfactant. Dependent variables included droplet size (Y_1), polydispersity index (Y_2), and cumulative drug release in 15 minutes (Y_3). The optimized formulation (X_1 = 10.0 mg, X_2 = 62.0 mg, X_3 = 40.0 mg) predicted Y_1, Y_2, and Y_3 values of 124.3 nm, 0.105, and 97.2%, respectively, with a desirability of 0.885 0. Pharmacokinetic studies showed that NMD-SNEDDS and MH-loaded NMD-SNEDDS increased oral bioavailability 3-fold and 4-fold, respectively, compared to pure drug suspension. MH-loaded NMD-SNEDDS demonstrated P-gp inhibition, enhancing NMD absorption. BBD effectively optimized the SNEDDS formulation, and MH-loaded NMD-SNEDDS is a promising approach to enhance NMD's oral bioavailability.

Keywords: nimodipine (NMD); morin hydrate (MH); self-nanoemulsifying drug delivery system (SNEDDS); Box–Behnken design (BBD); *in vivo* pharmacokinetic study; P-gp inhibition activity

Introduction

Subarachnoid hemorrhage (SAH) is a life-threatening condition where blood accumulates between the arachnoid and pia mater, often leading to cerebral vasospasm, a significant cause of death or disability. The incidence of SAH is approximately 10–14 per 100 000 person annually in the USA and 7.9 per 100 000 person annually worldwide [1–3]. Nimodipine (NMD), a dihydropyridine calcium antagonist, is the only Food and Drug Administration (FDA)-approved treatmentforvasospasmpost-SAH.Administeredorallyat 60 mg every 4 h, NMD reduces cerebral infarction and improves outcomes in patients following SAH, especially those without initial neurological deficits [4–6]. Despite its therapeutic potential, oral

administration of nimodipine (NMD) has limitations. As a Biopharmaceutical Classification System (BCS) Class II drug, NMD exhibits high permeability but poor solubility, resulting in low oral bioavailability (5%–13%). Extensive first-pass metabolism by CYP3A4 enzymes in the liver further reduces its systemic efficacy. Additionally, the P-glycoprotein efflux transporter in the small intestine limits NMD's bioavailability by actively transporting it out of enterocytes [7, 8].

Morin hydrate (MH), a flavonoid with antioxidant and anti-inflammatory properties, shows promise in enhancing NMD's bioavailability. Co-administration of MH with NMD may improve its bioavailability by modulating CYP3A4 and P-glycoprotein activity during first-pass metabolism, potentially increasing NMD's therapeutic effectiveness [9, 10]. Nanotechnology involves the study and application of nanoscale materials for manipulation, production, control, and utilization, driving the creation of revolutionary products with significant impacts on all aspects of life. Nanomedicines are developed to enhance the effectiveness of treatments for various debilitating diseases [11]. Self-nanoemulsifying drug delivery systems (SNEDDS) are lipid-based delivery systems designed to enhance the solubilization of highly lipophilic drugs [12, 13]. Comprising oils, surfactants, and cosurfactants, SNEDDS form oil-in-water nanoemulsions (20–200 nm) upon dilution in gastrointestinal fluids. These systems are easy to formulate, thermodynamically stable, and scalable, with high solvent capacity. SNEDDS improve drug permeation across the intestinal membrane, minimize food's impact on absorption, and protect drugs from acidic hydrolysis in the gastrointestinal (GI) tract by encapsulating them within the nanoemulsion's interior phase [14–16].

Quality by Design (QbD) is a strategic approach that utilizes systematic experimentation to identify and assess key variables affecting product quality and performance [17–19]. In QbD, Design of Experiments (DoE) and Response Surface Methodology (RSM) are employed to optimize products by ensuring the correct model is applied for optimal outcomes [20, 21]. RSM, a core element of QbD, is commonly used in experiments where multiple independent variables impact a dependent variable. The Box–Behnken Design (BBD), a specific type of RSM, is particularly effective in evaluating the effects of formulation variables and their interactions. BBD reduces the number of experimental runs by setting two factors at extreme values while centering the third. However, it may introduce errors when extrapolated to the design space extremes, making it most effective for non-linear relationships between factors and responses [22–24].

Nimodipine's oral bioavailability is limited due to poor solubility and extensive first-pass metabolism by CYP3A4, further restricted by the P-glycoprotein efflux transporter in the small intestine. To address this, a novel nano-formulation was developed to enhance NMD's solubility and bioavailability. The BBD was used to optimize a SNEDDS for NMD. Additionally, MH was incorporated into the optimized NMD-SNEDDS to further improve NMD's pharmacokinetic profile [25, 26].

In this study, the amounts of Capmul MCM (X_1), Cremophor RH-40 (X_2), and Transcutol P (X_3) were selected as independent variables. The BBD was employed to explore the main, interaction, and quadratic effects of these variables on droplet size (Y_1), polydispersity index (PDI) (Y_2), and the dissolution percentage of NMD after 15 min (Y_3). This research is the first to report the design and development of an MH-loaded NMD-SNEDDS aimed at enhancing the oral bioavailability of NMD in rats.

Experimental

Materials

NMD was received as a gift sample from Laksh Finechem Pvt. Ltd.(Anand, India). Gift samples of Acrysol were received from Corel Pharma (Ahmedabad, India), and Cremophor RH-40 (Polyoxyl 40 Hydrogenated Castor Oil USP/NF), Isopropyl Myristate, Oleic Acid, Olive Oil, Poloxamers, Solutol HS-15, Span 80, Triacetin, and Tween-80 from Sigma-Aldrich, Germany. Merck Pharmaceutical (Mumbai, India) donated Transcutol-P, and Gattefosse (India) donated Labrafac PG. Abitec Corporation (Mumbai, India) provided gift samples of Capmul MCM and Captex-300. Morin Hydrate was procured from Thermo Scientific Chemicals (USA). Aerosil® 200 Pharma (fumed silica) was purchased from Evonik Corporation, NJ. Verapamil was procured from Jai Radhe Sales

(Ahmedabad, India) and the PC-3 cell line was purchased from ACTREC (Mumbai, India). All solvents used in this research study were of analytical grade.

Solubility studies

The solubility of NMD in various oils, surfactants, and co-surfactants was assessed using the shake flask method across 17 different vehicles, as detailed in Table 1. For each test, excess NMD was added to 2 mL of the excipient in a microtube and mixed vigorously with a vortexer mixer for 5 min. The mixture was stabilized in a shaking water bath at 100 r/min and 25 °C for 48 h. It was then incubated in an environmental shaker bath at 37 °C with a shaking speed of 300 r/min for 72 h. After incubation, the samples were centrifuged at 15 000 r/min for 10 min to remove undissolved particles, and the clear supernatant was filtered through a 0.45 μm membrane filter. NMD concentration in the solutions was determined by high performance liquid chromatography (HPLC) analysis. The procedure was repeated 3 times to ensure accuracy and repeatability [27–31].

Screening of surfactant and co-surfactant (emulsification study)

Five surfactants (Tween-80, Cremophor RH-40, Tween-20, Acrysol K-150, and Solutol HS-15) were evaluated for emulsification efficiency using NMD solubility data. The main criterion was the surfactant's ability to emulsify the maximum amount of oil. A 15 wt.% surfactant solution in water was prepared, and 4 μL of oil, optimized from prior solubility studies, was added incrementally under vigorous vortexing to 2.5 mL of the surfactant solution. The process continued until a clear, single-phase solution was obtained, and additional oil was added until cloudiness occurred. The surfactant that emulsified the most oil without cloudiness was deemed optimal. Various co-surfactants (Transcutol-P, Triacetin, PEG-400, PEG-600, and propylene glycol (PG)) were assessed for emulsification effectiveness based on NMD solubility data. The key criterion was the ability to emulsify the largest amount of oil, guided by previous surfactant studies. A 15 wt.% mixture of surfactant and co-surfactant at a 1:1 ratio was prepared in water. To prepare this, 4 μL of oil was added incrementally with vigorous vortexing to

Table 1 Equilibrium solubility of NMD in various excipients.

Excipient	Solubility of NMD (mg/mL)	Excipient	Solubility of NMD (mg/mL)
Oils		**Surfactant**	
Captex 300	48.70 ± 0.613 3	Acrysol EL-135	13.13 ± 2.262 9
Soyabean oil	12.26 ± 1.443 1	Cremophor RH-40	46.72 ± 2.354 9
Corn oil	4.38 ± 0.223 8	Tween-20	36.17 ± 1.122 4
Capryol-90	59.56 ± 1.591 3	Acrysol K-140	6.43 ± 0.165
Capmul MCM	64.71 ± 0.284 5	Pluronic F-108	0.311 ± 0.013 4
Castor oil	16.43 ± 1.267 8	Pluronic F-127	0.245 ± 0.003 8
Oleic acid	15.33 ± 0.493 0	**Co-surfactant**	
Labrfac PG	55.97 ± 1.306 2	Span-80	13.24 ± 0.177 0
Isopropyl myristate	7.55 ± 0.848 5	PEG-600	4.88 ± 0.564 4
Olive oil	22.62 ± 0.975 3	Span-83	16.03 ± 0.613 5
Surfactant		Span-20	20.48 ± 0.332 7
Cremophor EL	12.72 ± 0.515 1	Propylene glycol	16.83 ± 0.537 5
Solutol HS-15	27.06 ± 0.506 7	Transcutol-P	76.52 ± 0.955 4
Acrysol K-160	14.36 ± 0.809 4	PEG-400	45.63 ± 1.582 2
Pluronic F-68	7.55 ± 0.414 1	Glyceryl triacetate	56.95 ± 1.165 9
Acrysol K-150	23.53 ± 1.036 8	PEG-200	14.94 ± 2.662 2
Pluronic M44	15.08 ± 0.741 8	4.5 pH acetate buffer	0.059 0 ± 0.006 0
Tween-80	54.36 ± 1.210 4	H_2O	0.002 62 ± 0.000 81

2.5 mL of the mixture until the solution became cloudy, indicating saturation. The co-surfactant that emulsified the most oil before cloudiness appeared was considered optimal [32, 33].

Construction of pseudo-ternary phase diagrams

Based on solubility and emulsification results, Capmul MCM, Cremophor RH-40, and Transcutol-P were chosen as the oil, surfactant, and co-surfactant, respectively, for formulation development. Pseudo-ternary phase diagrams of oil, surfactant/cosurfactant, and water were constructed using the aqueous titration method to obtain the maximal nanoemulsified oil percentage and the area of crystal liquid region. The basic SNEDDS formulation was selected to achieve a higher oil percentage and a smaller area of liquid crystal region. A ternary phase diagram was created to illustrate regions conducive to self-emulsification, excluding NMD due to the anhydrous nature of the SNEDDS. The visual test method assessed the formulations' ability to form nanoemulsions. For each phase diagram, oil and co-surfactant mixture (Smix) ratio (2:1) were mixed in different volume ratios ranging from 1:9 to 9:1 to obtain different combinations. The monophasic mixtures were slowly titrated with aliquots of water (37 ºC) and vortexed. After equilibrium was reached, the mixture was further titrated with aliquots of water until they showed the turbidity. The tendency to emulsify spontaneously and also the progress of emulsion droplets were observed visually, and the pseudo-ternary phase diagrams were constructed. The experiments were performed in triplicate. Based on the efficient self-nanoemulsifying region, the high, medium, and low levels of the independent variables were selected. The phase diagram boundaries established the ranges for the three independent factors (Capmul MCM (oil, X_1), Cremophor RH-40 (surfactant, X_2), and Transcutol-P (co-surfactant, X_3)) for the BBD. These ranges were 10–30 g for Capmul MCM, 40–70 g for Cremophor RH-40, and 20–40 g for Transcutol-P, as shown in Table 2 [34, 35].

Formulation of NMD-SNEDDS

The NMD-SNEDDS formulation was developed by incorporating the pure drug into a blank SNEDDS base, which consisted of oil, surfactant, and co-surfactant in a weight ratio of 100:10. NMD was gradually added to the oil phase while stirring continuously. This mixture was then added dropwise to a vial containing a pre-measured surfactant and Smix, which was prepared by blending the selected surfactant and co-surfactant in their specified ratios. The components were mixed thoroughly using gentle stirring and vortex mixing for 3 min, followed by sonication to enhance drug solubilization. The formulation was then agitated in a water bath at 37 °C with a 100 r/min setting for 48 h to ensure complete mixing, check for turbidity, and observe potential phase separation. Systematic optimization using QbD and response surface methodology was employed. Table 2 summarizes the formulation composition according to the BBD, outlining the influential factors. All formulations were evaluated for emulsification time, globule size, and *in vitro* drug release [36, 37].

Box–Behnken experiment design

A BBD with three factors and three levels was employed to explore and optimize the effects of formulation components on SNEDDS performance. This design requires 15 runs, including three central points, to assess experimental error and ensure accuracy. Fifteen experimental setups were created and analyzed using Minitab 17 software, facilitating a

Table 2 Variables in the Box–Behnken design.

	Levels		
Independent variable	**Low (−1)**	**Middle (0)**	**High (+1)**
X_1 = Amount of Capmul MCM added (mg)	10	20	30
X_2 = Amount of Cremophor RH-40 added (mg)	40	55	70
X_3 = Amount of Transcutol-P added (mg)	20	30	40
Dependent variables		**Goal**	
Y_1= Droplet size (nm)		Minimize	
Y_2= Polydispersity index (PDI)		Minimize	
Y_3= Dissolution percentage of NMD after 15 min		Maximize	

thorough optimization of the SNEDDS formulation. Table 3 shows the 15 randomized experimental runs and their responses from the BBD [38, 39].

Based on the ternary phase diagram, the chosen ranges for the SNEDDS components were: oil (10–30 g), surfactant (40–70 g), and co-surfactant (20–40 g). Key response factors were identified to assess the quality of the SNEDDS formulation, including droplet size (Y_1), polydispersity index (Y_2), and the dissolution percentage of NMD after 15 min (Y_3), as detailed in Table 2. The data for each response factor were modeled using a quadratic polynomial equation:

$$Y = \beta_0 + \beta_1 X_1 + \beta_2 X_2 + \beta_3 X_3 + \beta_4 X_1 X_2 + \beta_5 X_2 X_3 + \beta_6 X_1 X_3 + \beta_7 X_1^2 + \beta_8 X_2^2 + \beta_9 X_2^2 \quad (1)$$

In this equation, Y represents the measured response; $\beta_0 - \beta_9$ are the regression coefficients; and X_1, X_2, and X_3 symbolize the independent factors. The adequacy and reliability of the models were confirmed through analysis of variance (ANOVA), tests for lack of fit, and determination of the multiple correlation coefficient (R^2), ensuring a robust evaluation of the SNEDDS formulation's performance [40].

Optimization using the desirability function

To optimize multiple responses effectively, strong correlations among them are essential. However, the optimal conditions for one response may conflict with those for another, making it necessary to find a compromise. This study used a comprehensive approach to simultaneously optimize all three responses through a desirability function. This method, implemented using Minitab 17 software, applies numerical optimization techniques. The desirability function, commonly used in recent publications for multi-response optimization, is a robust tool for identifying balanced conditions across different response variables [41, 42]. In the desirability function approach, each response is assigned a specific target, and multiple response criteria are combined into a single criterion problem. This is done by associating each response with its partial desirability function. Responses are rated between 0 and 1, with 0 for unacceptable responses and values closer to 1 for those nearer to the target. Responses outside the acceptable range are deemed unacceptable. Individual desirability values are combined using a geometric mean to obtain an overall desirability value (D). Minitab 17 then performs a grid search to find the maximum desirability value based on the goals for all responses.

Preparation of MH-loaded NMD-SNEDDS

Optimized formulation of NMD-SNEDDS was used to prepare MH-loaded NMD-SNEDDS. MH was

Table 3 Experimental matrix and observed responses from randomized runs in the Box–Behnken design.

Batch Number	Independent Variables			Dependent Variables		
	X_1 = Capmul MCM (mg)	X_2 = Cremophor RH-40 (mg)	X_3 = Transcutol-P (mg)	Y_1= Droplet size (nm)	Y_2= Polydispersity index (PDI)	Y_3= Dissolution percentage of NMD after 15 min
BBD1	20	40	40	163.5	0.220	65.8
BBD2	30	55	40	145.9	0.212	91.7
BBD3	20	40	20	168.5	0.125	80.6
BBD4	10	40	30	130.5	0.165	69.8
BBD5	10	70	30	140.6	0.081	95.8
BBD6	20	55	30	127.6	0.156	96.5
BBD7	30	55	20	137.6	0.198	91.4
BBD8	20	55	30	138.4	0.122	89.5
BBD9	10	55	40	116.4	0.147	94.6
BBD10	30	70	30	103.6	0.192	97.2
BBD11	30	40	30	281.4	0.319	78.2
BBD12	20	70	20	71.6	0.290	91.2
BBD13	20	70	40	106.5	0.172	95.1
BBD14	10	55	20	98.4	0.191	96.3
BBD15	20	55	30	134.6	0.265	88.5

incorporated into SNEDDS with an objective to improve the overall oral bioavability of NMD. MH was added with the weight ratio of NMD: MH of 1:1. The desired amount of MH was added to optimized formulation of NMD-SNEDDS and homogenized until a transparent homogenous system was formed [43].

Characterization of SNEDDS

Determination of droplet size, polydispersity index, zeta potential and drug content

Fifteen liquid SNEDDS formulations, each containing 10wt.% NMD, were prepared using DoE. A 100 µg sample from each formulation was diluted in 100 mL of deionized water at 37 °C and gently stirred with a magnetic stirrer. The droplet size of the emulsion was immediately measured using a Zetatrac instrument (Microtrac, USA) at a wavelength and scattering angle of 90°, maintained at 25 °C. Measurements were taken in triplicate, and the z-average diameters were calculated. The software also provided the PDI and zeta potential for both the optimized NMD-SNEDDS and MH-loaded NMD-SNEDDS formulations [44, 45].

Self-emulsification time and precipitation assessment

The emulsification time for each batch of SNEDDS, optimized NMD-SNEDDS, and MH-loaded NMD-SNEDDS was determined using a USP type II (paddle method) dissolution apparatus. Each 0.5 mL formulation was gradually added to 500 mL of 0.1 mol/L HCl at (37 ± 2) °C, with the paddle stirring at 50 r/min. The time required to form a homogeneous dispersion was noted and considered the self-emulsification time. Emulsion stability was visually assessed after 48 h of storage at room temperature, categorizing formulations as clear (transparent or bluish) or non-clear (turbid), and stable (no precipitation) or unstable (precipitation). All experiments were conducted in triplicate, and formulations without drug precipitation or phase separation were deemed “robust” to dilution [32].

Refractive index and percentage transmittance

The isotropy of all experimental designs, including the optimized NMD-SNEDDS and MH-loaded NMD-SNEDDS (diluted 1 000 times with distilled water), was assessed using refractive index (RI) measurements. A drop of each formulation was placed on a refractometer slide, and the RI was measured in triplicate, with mean values recorded. Optical clarity of the batches was quantified by measuring percentage transmittance (*T*%) spectrophotometrically. Each batch was diluted 1 000 times in distilled water, allowed to stand for 2 h, and *T*% was measured at 650 nm using a double-beam ultraviolet (UV) spectrophotometer. Distilled water served as the blank, and the analysis was conducted on three independent samples, with mean values documented [46].

In vitro dissolution study

An *in vitro* drug release study was conducted using a USP type-II dissolution test apparatus (Electro lab TDT-06P, India). The dissolution medium comprised 900 mL of water, maintained at (37 ± 0.5) °C and stirred at 50 r/min. Each SNEDDS formulation, containing 30 mg of NMD, was encapsulated in a size "0" hard gelatin capsule (HGC) with colloidal silica (Aerosil® 200) as the inert carrier. For comparison, 30 mg of NMD powder was similarly encapsulated, and a dissolution study was performed. Capsule sinkers ensured the capsules remained submerged. Aliquots of 5 mL were withdrawn at intervals of 5, 10, 15, 20, 30, and 60 min, and the volume was replenished with fresh medium. The samples were filtered through a 0.45 µm Whatman filter paper and analyzed for NMD content using HPLC. Additionally, the dissolution profiles of optimized NMD-SNEDDS and MH-loaded NMD-SNEDDS were separately evaluated in pH 4.5 acetate buffer, pH 6.8 phosphate buffer, and water to determine the influence of physiological pH on dissolution behavior. Each test was replicated three times with independent samples, and average values were used to generate the dissolution profiles [47, 48].

Robustness to dilution

The robustness of the optimized NMD-SNEDDS and MH-loaded NMD-SNEDDS was tested by diluting the formulations 100-fold with various media, including 0.1 mol/L HCl, water, and buffers at pH 4.5, 6.8, and 7.4. The impact of dilution was evaluated by measuring changes in globule size. Samples of the diluted SNEDDS were stored for 48 hours to monitor for phase separation or drug precipitation. The study, conducted in triplicate, provided insights into the stability of the NMD-loaded SNEDDS at infinite dilution [49].

Differential scanning calorimetry (DSC) analysis

DSC is a widely recognized thermal analysis technique for assessing drug-excipient compatibility. Known for its efficiency and flexibility, DSC requires only milligram-sized samples to detect heat changes as a sample undergoes physical or chemical transitions with temperature. In this study, DSC analysis was conducted using a Shimadzu DSC-60. Samples were heated from 30 to 300 °C at a rate of 10 °C per min in a nitrogen atmosphere (40 mL/min). Thermograms were generated for pure NMD, morin hydrate, their physical mixture with excipients, optimized NMD-loaded SNEDDS, and morin hydrate-loaded NMD-SNEDDS [50].

Fourier Transform infrared spectrometer (FTIR) analysis

FTIR spectroscopy is an indispensable analytical technique renowned for its effectiveness in chemical identification. It plays a pivotal role in drug-excipient compatibility studies by detecting interactions between the drug and chosen excipients within a formulation. For this purpose, infrared spectra of pure drug NMD, MH, a physical mixture of NMD with excipients, optimized NMD-SNEDDS, and MH-loaded NMD-SNEDDS were recorded. The scanning was conducted using an FTIR 8400S spectrometer (Shimadzu, Japan) over a spectral range of 4 000 to 400 cm^{-1} [51].

Morphological observation

Morphological and structural analysis of the optimized MH-loaded NMD-SNEDDS was conducted using transmission electron microscopy (TEM; Technai-20, Phillips and Holland) at an accelerating voltage of 100 kV. A droplet (0.8 mL) of the SNEDDS formulation, diluted 1:100 with water, was directly placed on copper electron microscopy grids coated with formvar films. The grids were then stained with a 0.5% aqueous solution of phosphotungstic acid (2%, w/v) for 30 s. After drying, the grids were examined using TEM. Various bright-field imaging techniques at increasing magnifications were employed to reveal the structure and size of the resulting nanoemulsion [52].

Cell viability

The potential cytotoxicity of NMD-SNEDDS and MH-loaded NMD-SNEDDS was assessed using the MTT (3-(4,5-dimethylthiazol-2-yl)-2,5-diphenyltetrazolium bromide) assay. Caco-2 cells were routinely cultured and prepared for the test. After removing the old media, the cells were rinsed with phosphate buffered saline (PBS, pH 7.4) and treated with 1 000 μL of trypsin (0.25% Trypsin-EDTA). Fresh, complete Dulbecco's modified eagle medium (DMEM) containing pre-warmed FBS, penicillin (10 000 units/mL), streptomycin (10 000 μg/mL), and L-glutamine 100 mmol/L (100×) was then added. The cells were incubated at 37 °C in a humidified atmosphere with 5%CO_2. Caco-2 cells with passage numbers between 20 and 30, exhibiting optimal growth, were seeded for the cytotoxicity evaluation.

Cell growth for the MTT assay was monitored under a microscope, and 10 μL of cell suspension (9 000–10 000 cells per well) was plated into a 96-well plate. Each well was treated with 10 μL of either control or sample solutions at varying concentrations (0, 0.025, 0.05, 0.075, 0.1, 0.25, 0.5%, v/v) in complete medium. For higher concentrations of NMD (250 and 500 μmol/L), a small amount of DMSO (< 1% v/v) was added to the medium to enhance solubility. Following a 24-h incubation, the media was replaced with MTT solution (0.5 mg/mL) and incubated for an additional 3 h at 37 °C in the dark. The MTT solution was then replaced with dimethylsulfoxide (DMSO), and the absorbance of each well was measured at 570 nm using a microplate reader. Cell viability was calculated as a percentage relative to the control [53].

In vivo pharmacokinetic studies

In vivo pharmacokinetic studies were conducted on male Sprague–Dawley rats (200 ± 20) g. The rats were housed individually at (25 ± 2) °C with 45% ± 5% relative humidity for a week before the experiments. 24 rats were randomly divided into 4 groups of 6. Before the experiments, the rats were fasted for 10–12 h with water available. The control group received a suspension of NMD with 1% polyvinylpyrrolidone K30 in water. Test groups were orally administered either optimized NMD-SNEDDS, MH-loaded NMD-SNEDDS, or a marketed nimodipine suspension, all at a dosage of 20 mg/kg. Each rat was anesthetized in an ether-saturated chamber and placed supine on a surgical board. A cannula, pre-flushed with heparinized saline (80 IU), was inserted into the femoral artery for blood

collection via a three-way stopcock. Blood samples (200 μL) were taken at 0.25, 0.5, 1, 2, 4, 6, 8, 10, and 12 h. Plasma was separated by centrifugation at 3 000 r/min for 10 min and stored at –40 °C until analysis. All procedures were conducted under reduced light to prevent nimodipine photo-degradation, in accordance with Institutional Animal Ethics Committee (IAEC) guidelines, CPCSEA, Government of India. Nimodipine concentration in blood was measured using reverse-phase HPLC. Plasma samples were processed by mixing 200 μL of plasma with 25 μL of internal standard solution (amlodipine, 2 ng/mL in methanol), followed by vortexing, extraction, evaporation, and dissolution before HPLC analysis. Pharmacokinetic parameters (C_{max}, T_{max}, and AUC) were calculated using standard non-compartmental analysis. The relative bioavailability of the optimized SNEDDS versus the suspension was assessed, with significant differences evaluated using Student's t-tests (mean ± SD, $p < 0.05$) [54].

Study of P-glycoprotein inhibition activity

The impact of NMD-SNEDDS, MH-loaded NMD-SNEDDS, and paclitaxel on PC-3 cell growth was evaluated using the MTT assay, with Verapamil, a P-glycoprotein (P-gp) substrate, included in the experiments. Three separate experiments were conducted. First, PC-3 cells were treated with varying concentrations (0.50–50 μg/mL) of NMD-SNEDDS and MH-loaded NMD-SNEDDS to determine their IC_{10} values. Second, different concentrations of Verapamil (50–200 μg/mL) were applied to PC-3 cells to establish its IC_{50} value. Finally, PC-3 cells were exposed to various Verapamil concentrations (30–200 μg/mL) in the presence of the IC_{10} concentration of NMD-SNEDDS and MH-loaded NMD-SNEDDS to evaluate any potential alteration in Verapamil's IC_{50}, aiming to detect any inhibitory effect on P-gp. The IC_{50} and IC_{10} values were calculated using the linearized form of the median effect equation:

$$\log (F_a/F_u) = m\log (D) - m\log (D_{med}) \quad (2)$$

where D is the dose; F_a and F_u are the fractions of the system affected and unaffected, respectively, by the dose D; D_{med} is the dose required to produce the median effect (IC_{50}), and m is a Hill-type coefficient signifying the sigmoidicity of the dose–effect curve [55].

Stability study

Accelerated stability studies were conducted on the optimized NMD-SNEDDS and MH-loaded NMD-SNEDDS formulations to evaluate stability and estimate shelf life, following the ICH Q1A (R2) guidelines (2003). The formulations, encapsulated in hard gelatin shells, were stored in amber glass containers under accelerated conditions ((40 ± 2) °C/(75 ± 5) RH%) for 6 months. Intermediate testing at 0, 3, and 6 months assessed drug assay (%), drug release (%) over 15 min, particle size (nm), PDI, zeta potential (mV), percentage transmittance (T%), and emulsification time. Drug assay data were plotted against time and extrapolated using Sigma Plot 12.5 software to determine the shelf life (t_{90}) of the formulations [56].

Results and Discussion

Solubility studies

A crucial aspect of developing SNEDDS is selecting the oil phase, which plays a significant role in the drug's dissolution rate and absorption in the gastrointestinal tract. Solubility studies are essential for identifying oils, surfactants, and co-surfactants that maximize drug solubility, enabling optimal drug loading and efficient emulsification. In this study, a saturation solubility analysis was conducted to identify excipients capable of solubilizing a significant amount of NMD, with the results detailed in Table 1. NMD exhibited maximum solubility in Capmul MCM, Tween-80, and Transcutol-P, with solubility values of 64.71, 54.36, and 76.52 mg/mL, respectively. Various surfactants and co-surfactants were evaluated based on their solubility and emulsification abilities, ensuring they could effectively emulsify the oil phase while maintaining high drug solubility. Capmul MCM, which demonstrated the highest solubility for NMD among the tested oils, was selected for the NMD-SNEDDS formulation. Its high drug solubility reduces the amount of oil required, thereby minimizing the need for surfactants and co-surfactants to emulsify the drug-loaded oil droplets. Capmul MCM, a blend of medium-chain mono- and di-glycerides with a hydrophilic–lipophilic balance (HLB) value of 4.7, is commonly used in lipid-based drug delivery systems (LBDDS) due to its ability to enhance the solubility of poorly soluble drugs, increasing drug-loading

capacity. Previous research has shown that the inclusion of Capmul MCM, which contains polar hydroxyl groups, significantly improves drug solubility, as demonstrated with drugs like Danazol [57, 58]. Therefore, selecting excipients that enhance drug solubility is essential for preventing drug precipitation during storage and improving both *in vitro* and *in vivo* drug performance, leading to optimal absorption.

Screening of surfactant and co-surfactant (emulsification study)

In this study, the selection of surfactants and co-surfactants was driven by their emulsification efficiency rather than just their ability to solubilize NMD. While a surfactant might excel at drug solubilization, it doesn't necessarily perform well in emulsifying oil. Therefore, we evaluated surfactants with HLB values ranging from 6 to 16 for their dual abilities: solubilizing the drug and effectively emulsifying the selected oil phase [52, 53]. The screening process prioritized surfactants capable of emulsifying the maximum amount of oil, as an ideal SNEDDS should rapidly form a nano-sized, transparent emulsion under gentle agitation. Among the tested surfactants, Cremophor RH-40 demonstrated the highest oil solubilization capacity at 3.84% (w/w) ($p < 0.001$) (Fig. 1(a)), making it the optimal choice for further study. Although some surfactants showed effective drug solubilization, they had limited oil emulsification capabilities. This finding suggests that high drug solubility in a surfactant doesn't automatically translate into effective oil emulsification. Cremophor RH-40's superior performance likely stems from its higher affinity for the oil phase and its structural properties, such as chain length, which enhance its emulsification capacity. Cremophor RH-40 was selected over Tween-80 due to its superior oil emulsification, which is crucial for creating a stable SNEDDS. While Tween-80 offered better drug solubility, effective emulsification is key for enhancing bioavailability. Cremophor RH-40 ensures rapid and complete oil dispersion, improving absorption efficiency, making it the preferred choice for this formulation.

Next, five co-surfactants were tested in combination with Cremophor RH-40 at a 1:1 ratio. The hydrophilic co-surfactants (Transcutol P, PEG 400, PEG 600, and PG) exhibited better emulsification of the selected oil phases compared to the lipophilic co-surfactant, Triacetin. Transcutol P stood out by achieving the highest emulsification, and solubility studies further confirmed its excellent NMD solubility (Fig. 1(b)). This advantage led to the selection of Transcutol P as the co-surfactant for all subsequent NMD trials. For effective nanoemulsion formulation, the chosen surfactant must significantly reduce interfacial tension and facilitate dispersion while possessing appropriate lipophilic characteristics for proper curvature at the oil-water interface. In this study, non-ionic surfactants were preferred due to their pH insensitivity, safety, biocompatibility, and enhanced emulsion stability. Incorporating an appropriate co-surfactant in SNEDDS formulations is crucial for reducing interfacial tension, fluidizing the hydrocarbon region of the interfacial film, and decreasing bending stress. This enhances the spontaneity of emulsification, reduces globule size and polydispersity, and improves thermodynamic stability by lowering interfacial energy and providing a mechanical barrier to coalescence [19–21].

Construction of pseudo-ternary phase diagrams

The relationship between the phase behavior and composition of SNEDDS mixtures was explored using pseudo-ternary phase diagrams, which were

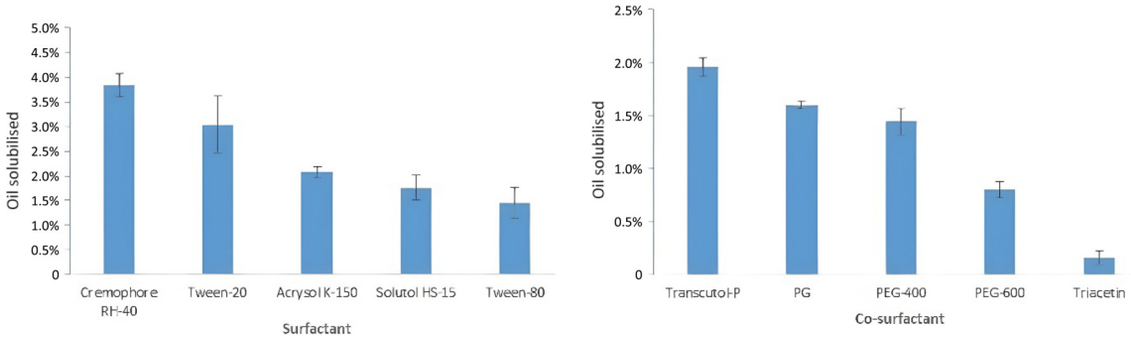

Fig. 1 Screening of **(a)** Surfactant and **(b)** Co-surfactant with oil solubilisation capacity.

constructed without NMD to identify self-emulsifying regions and optimize the proportions of oil, surfactant, and co-surfactant in SNEDDS formulations. Specifically, these diagrams (Fig. 2) were created for systems containing Capmul MCM as the oil, Cremophor RH-40 as the surfactant, and Transcutol-P as the co-surfactant. The largest self-emulsifying region was found at a Smix (Cremophor RH-40: Transcutol P) ratio of 2:1. Shaded areas in the diagrams indicate nanoemulsification zones likely to produce globules smaller than 100 nm, while the surrounding regions represent formulations with poor emulsification and larger globule sizes. The boundary between the shaded (nanoemulsion) and white (poor emulsification) regions in the ternary phase diagram was determined based on visual observation and droplet size measurements. "Poor" emulsification is characterized by incomplete or slow dispersion upon dilution, along with phase separation. Droplet size distribution in the nanoemulsion region is typically around 100 nm, ensuring better stability and absorption. A Smix ratio of 2:1 and an oil ratio of 1:4 produced extensive nanoemulsion regions. These observations were used to determine the range or levels of independent variables (amounts of SNEDDS components) for further study. The self-emulsifying region initially expanded as the surfactant to co-surfactant ratio increased, due to the enhanced adsorption of surfactant molecules at the oil-water interface, which lowers interfacial tension and facilitates the formation of smaller droplets. However, at higher surfactant concentrations, the self-emulsifying area decreased because of the formation of a highly viscous liquid crystalline phase, which hinders the spontaneous breakup of the interface [37].

Box–Behnken design

A three-factor, three-level BBD was employed to evaluate the effects of independent variables on three critical responses: droplet size (Y_1), polydispersity index (PDI, Y_2), and drug release percentage after 15 minutes (Y_3) in the NMD-SNEDDS formulation. The design layout and results for 15 experiments are presented in Table 3. Data analysis was conducted using Minitab® 17 software, modeling each response with a second-order quadratic equation. Model significance was determined through analysis of variance (ANOVA), lack-of-fit tests, and calculation of the multiple correlation coefficient (R^2). A model is considered well-fitting if the p-value is less than 0.05. The lack-of-fit test, with a p-value greater than 0.1, indicates that deviations from the model are insignificant relative to the pure error, suggesting a good fit. A significant lack-of-fit indicates poor predictive capability of the model [14, 40]. The multiple correlation coefficient (R^2) reflects how well the model explains the variation in the response, with R^2 values over 0.7 considered acceptable and values above 0.9 deemed excellent. Table 4 presents the results, including model p-values, individual term p-

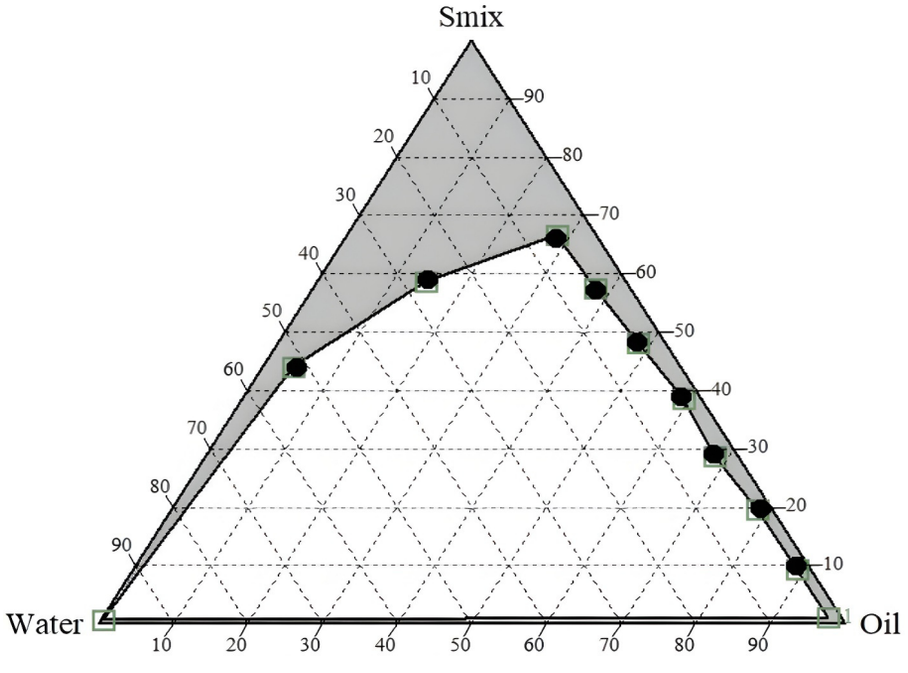

Fig. 2 The pseudo-ternary phase diagram indicating o/w nanoemulsion region at 2:1 Smix ratio.

values, lack-of-fit tests, and R^2 values for each response. In the ANOVA, model *p*-values for Y_1 (droplet size), Y_2 (PDI), and Y_3 (NMD dissolution after 15 min) were all below 0.05, confirming that each response was well-fitted by the quadratic model. The lack-of-fit tests yielded *p*-values of 0.290 8, 0.621 5, and 0.136 9, respectively, indicating no significant lack-of-fit ($p > 0.1$) for all variables (Y_1, Y_2, and Y_3), suggesting the models are adequate with no significant discrepancies between observed and predicted values. Additionally, the R^2 values for Y_1, Y_2, and Y_3 were 0.985 7, 0.978 5, and 0.964 5, respectively, indicating a high level of confidence (> 96%) in the regression equations' ability to predict observed values accurately. Table 4 also lists coefficients, including factor intercepts, interaction terms (X_1X_2, X_1X_3, and X_2X_3), and higher-order effects (X_1^2, X_2^2, and X_3^2), highlighting significant interaction and quadratic effects within the model.

Influence of independent variables on globule size

The size of nanoemulsion (NE) globules critically affects drug release, permeation through the stratum corneum, and retention in the epidermis and dermis, making it essential to formulate NEs with a mean globule size under 200 nm. ANOVA analysis of the experimental results showed a high coefficient of determination (R^2 = 0.985 7) for the quadratic model. Additionally, the quadratic model had the lowest predicted residual sum of squares (PRESS) compared to the linear and 2FI models, indicating its suitability.

Table 4 Statistical analysis of measured responses.

Fitting model	Factors	Coefficient	*p*-value	ANOVA
Droplet size	Intercept	231.5		F = 31.460 0, R^2 = 0.985 7 Model *p*-value < 0.000 1 *p*-value of lack-of-fit = 0.290 8
	X_1	65.654	< 0.000 1	
	X_2	–49.573	< 0.000 1	
	X_3	–6.528	0.024 8	
	X_1X_2	–8.42	0.074 8	
	X_1X_3	22.4	0.035 2	
	X_2X_3	–0.425	0.857 1	
	X_1^2	–2.328 5	0.441 8	
	X_2^2	15.142 7	0.145 8	
	X_3^2	–2.547 2	0.274 5	
PDI	Intercept	0.1578		F = 18.698 7, R^2 = 0.978 5 Model *p*-value < 0.000 3 *p*-value of lack-of-fit = 0.621 5
	X_1	–0.024 78	0.001 6	
	X_2	–0.021 8	0.003 9	
	X_3	–0.007 1	0.112 6	
	X_1X_2	0.004 9	0.654 8	
	X_1X_3	–0.031 0	0.016 8	
	X_2X_3	–0.002 9	0.795 4	
	X_1^2	0.077 2	<0.000 1	
	X_2^2	–0.018 5	0.054 8	
	X_3^2	0.040 3	0.001 3	
Dissolution percentage of NMD after 15 min	Intercept	82.598 7		F = 24.1068, R^2 = 0.9645 Model *p*-value < 0.0002 *p*-value of lack-of-fit = 0.1369
	X_1	–6.587 4	0.004 8	
	X_2	1.265 8	0.520 1	
	X_3	12.659 8	<0.000 1	
	X_1X_2	–3.587 1	0.169 7	
	X_1X_3	15.987 2	0.001 5	
	X_2X_3	16.987 5	0.000 7	
	X_1^2	–1.039 8	0.651 4	
	X_2^2	–15.698 7	0.000 1	
	X_3^2	–8.987 5	0.004 3	

The model's significance is supported by an F-value of 31.460 0 (Table 4), with all independent variables significantly influencing droplet size ($p < 0.05$). The amount of oil (X_1) and surfactant (X_2) had a more pronounced effect on droplet size than the amount of co-surfactant (X_3). However, a significant interaction between co-surfactant and oil (p-value $X_1X_3 < 0.05$) was observed in influencing nanoemulsion droplet size. Increasing X_1 resulted in larger droplet sizes, while higher amounts of X_2 and X_3 reduced droplet size. 3D response surface plots illustrating these relationships are depicted in (Fig. 3(a)). The 3D response surface and contour plots revealed that lower concentrations of surfactant and co-surfactant led to larger globule sizes, likely due to non-uniform film formation around oil droplets, causing fusion. Conversely, higher surfactant and co-surfactant concentrations reduced interfacial tension between the oil and water phases, lowering the energy required to disrupt droplets, thereby significantly reducing globule size. The formation of a complex film around oil globules further inhibited coalescence. At higher surfactant and co-surfactant levels, globule size became primarily dependent on oil concentration. These findings align with previous studies, which reported significant reductions in nanoemulsion globule size with increased surfactant concentration, supporting the principles of self-emulsification theory

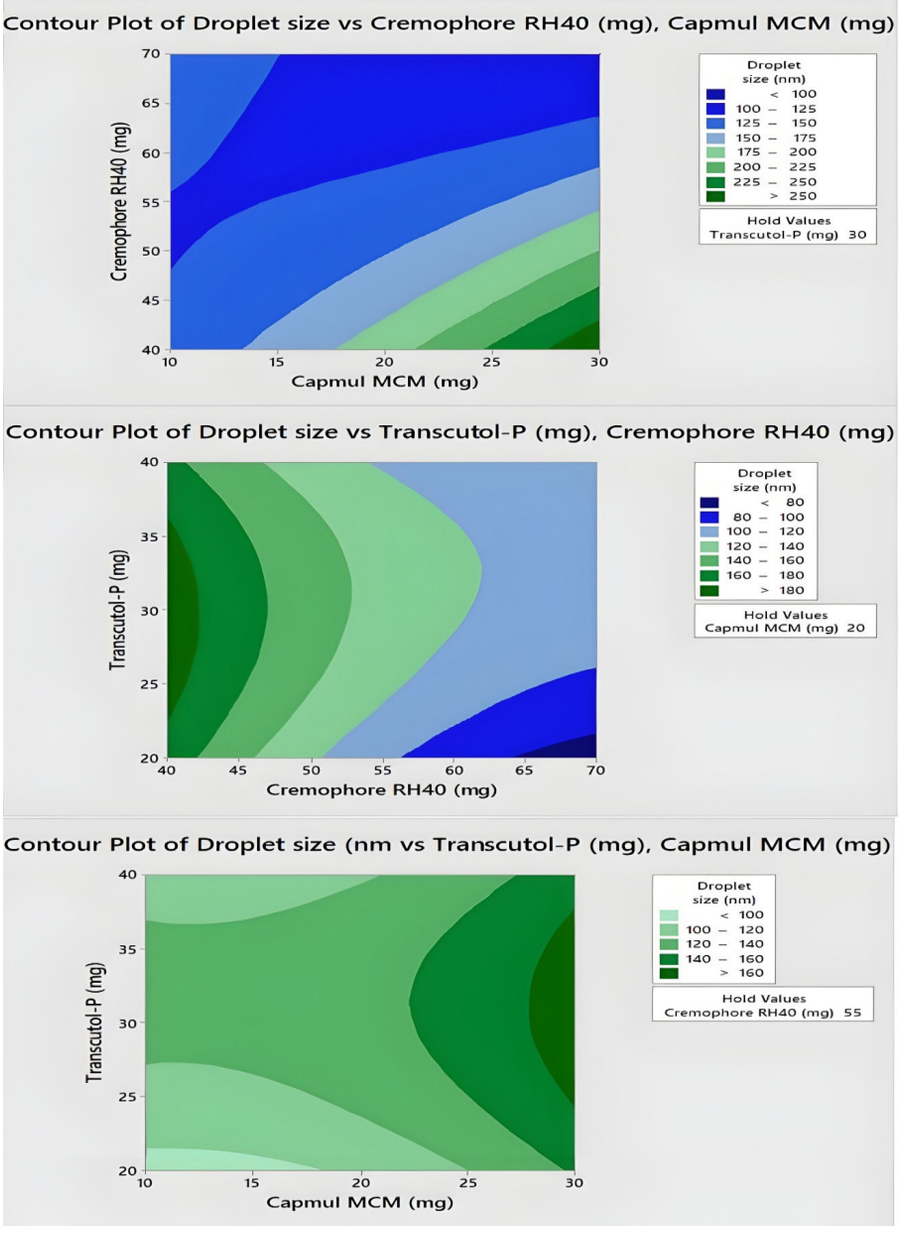

Fig. 3 3D response surface plots for droplet size (nm).

[59].

Influence of independent variables on PDI

The PDI indicates the size distribution of nanoemulsion droplets formed by SNEDDS, offering insight into the uniformity of droplet sizes. ANOVA analysis and model summary statistics revealed a high R^2 value (0.978 5) for the quadratic model, along with the lowest PRESS compared to linear and 2FI models. These results suggest that the quadratic model fits the data well. PDI was significantly influenced by the amount of oil (X_1), surfactant (X_2), the interaction between oil and co-surfactant (X_1X_3), and the quadratic terms for oil (X_1^2) and co-surfactant (X_3^2) ($p < 0.05$). The model's F-value of 18.698 7 indicates its significance, with the quadratic interaction of X_1^2 showing the most substantial effect. The 3D response surface (Fig 4(a)) showed that increasing oil concentration significantly raised the PDI value. In contrast, higher concentrations of surfactant and co-surfactant decreased the PDI value, resulting in a narrower globule size distribution. However, at high oil concentrations, the surfactant and co-surfactant were insufficient to micellize the droplets, causing globule fusion and increasing the PDI [60].

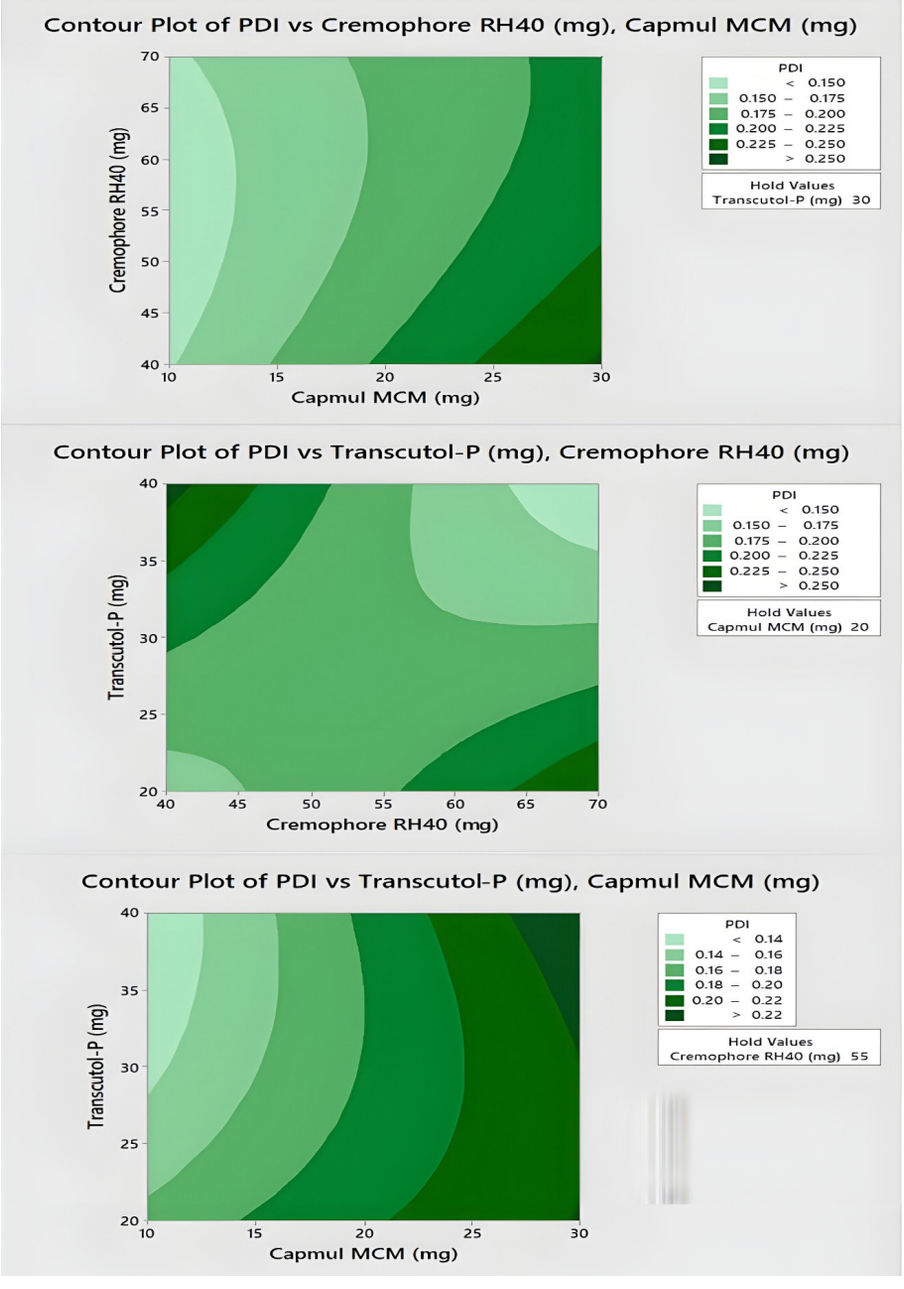

Fig. 4 3D response surface plots for PDI.

Influence of independent variables on dissolution percentage of NMD after 15 min

The total drug content in all formulations ranged from (88.47% ± 0.37%) to (96.24% ± 0.47%), demonstrating robust NMD loading capacity. The percentage of drug release after 15 minutes varied between 56.97% and 95.63%. ANOVA analysis showed a high R^2 value of 0.964 5 for the quadratic model, with the lowest PRESS value compared to linear and 2FI models. These results indicate that the quadratic model fits the data well, with a significant Model F-value of 24.106 8.

The amount of oil (X_1) and co-surfactant (X_3) significantly affected the percentage of drug release after 15 minutes (p-value < 0.05). Although the amount of surfactant (X_2) did not directly impact drug release, its interaction with co-surfactant (X_2X_3) had a greater effect than X_1 and X_3. The quadratic effect of X_2 had a notable negative impact on drug release (coefficient = −17.951, p < 0.000 2). 3D response surface (Fig. 5(a)) indicated that increasing surfactant and co-surfactant concentrations improved NMD dissolution, while higher oil concentrations reduced drug release. Balancing surfactant and co-surfactant concentrations enhances drug release and emulsion stability [55].

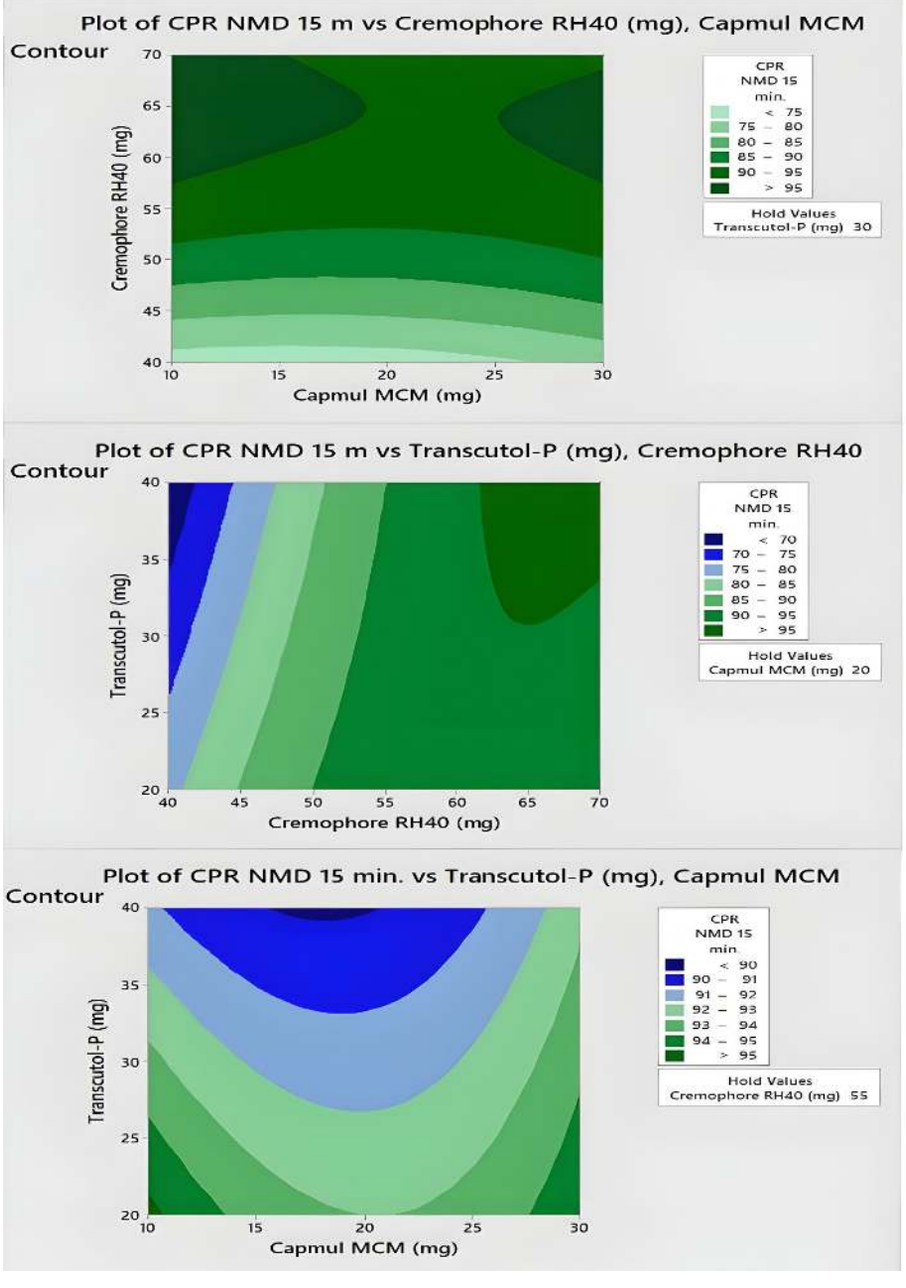

Fig. 5 3D response surface plots % dissolution of NMD in 15 min.

Optimization using desirability function

The optimized NMD-SNEDDS formulation was achieved through a desirability function aimed at simultaneously minimizing droplet size and PDI while maximizing drug release after 15 minutes. This multi-response optimization process converts multiple responses into a single objective using mathematical calculations [24]. The target for globule size (Y_1) was set between 50–200 nm to enhance skin permeation, as particles smaller than 200 nm improve drug delivery. PDI (Y_2) was minimized, and the percentage of drug dissolution after 15 minutes (Y_3) was targeted to exceed 85% to ensure a monodisperse nanoemulsion and high drug entrapment. The second-order quadratic model's response surface is shown in Fig. 6, with optimal levels for oil (X_1), surfactant (X_2), and co-surfactant (X_3) at 10.0 mg, 62.0 mg, and 40.0 mg, respectively. Predicted values were 124.3 nm for globule size, 0.105 for PDI, and 97.2% for drug release, with a desirability of 0.885 0. The experimental results, shown in Table 5, closely match the predicted values, validating the accuracy of the BBD and desirability function in the optimization process. The percent bias was between –4.68% and +2.94%.

Characterization of SNEDDS

Determination of zeta potential and drug content

The zeta potential values for the NMD-SNEDDS formulations ranged from –12.70 to –18.12 mV, indicating moderate electrostatic stability, as shown in Table 6. These values suggest that while the formulations do not reach the threshold of –30 mV typically associated with high stability, they are stabilized through steric effects provided by the surfactants. Cremophor RH-40, a non-ionic surfactant, creates a steric barrier around the droplets, preventing aggregation, although it does not significantly alter the zeta potential. Transcutol-P, while not affecting the zeta potential alone, enhances stability and solubility in combination with Cremophor RH-40. Thus, despite the moderate zeta potentials, the formulations remain stable due to the steric stabilization and improved solubilization. Zeta potential is critical for assessing the stability, dispersion, and interaction of nanoemulsions with biological membranes [32, 19]. A higher absolute zeta potential generally indicates better stability and reduced aggregation. Cremophor RH-40 is a highly effective non-ionic surfactant known for its excellent

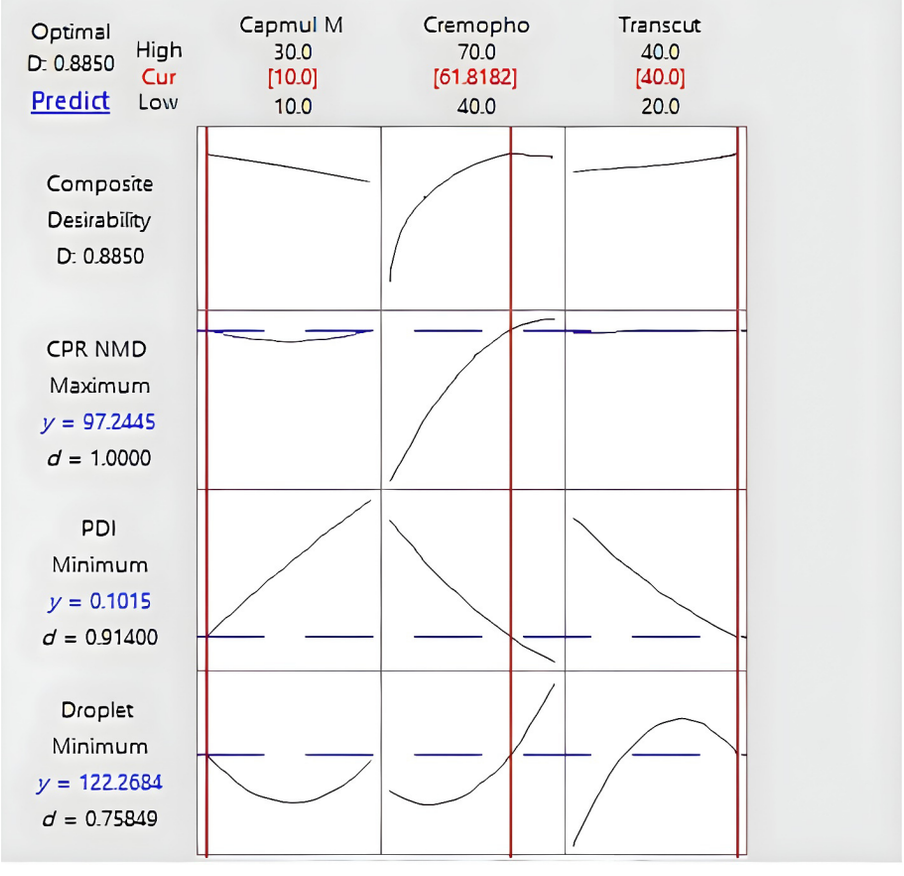

Fig. 6 Optimization plot representing values of responses.

Table 5 The predicted and observed values of optimized NMD-SNEDDS

Responses	Predicted value	Observed value	Bias
Y_1	124.3 nm	130.4 ± 0.9 nm	–4.68%
Y_2	0.105	0.102 ± 0.012	2.94%
Y_3	97.2%	95.6% ± 1.2%	1.67%

solubilizing properties, enhancing the dispersion of lipophilic drugs like NMD within SNEDDS. It increases the drug loading capacity by improving nimodipine's solubility, allowing higher concentrations without precipitation. Transcutol-P, acting as both a co-surfactant and solubilizer, aids in partitioning nimodipine into the oil phase, which helps maintain high drug content and stability in the SNEDDS. These excipients stabilize nimodipine in the nanoemulsion, preventing precipitation and ensuring solubility throughout the product's shelf life. The drug content in NMD-SNEDDS formulations ranged from 92.54% to 97.85%, indicating uniform dispersion. HPLC analysis of optimized NMD-SNEDDS and MH-loaded NMD-SNEDDS showed high precision, with drug contents of 94.9% ± 0.3% and 92.5% ± 0.2%, respectively.

Self-emulsification and precipitation assessment

Emulsification studies are an essential method for evaluating the self-emulsifying properties of developed formulations. SEDDS should rapidly and fully disperse upon aqueous dilution with gentle agitation. The surfactants in SEDDS lower the interfacial tension between the oil and water phases, promoting dispersion and the formation of oil-in-water emulsions. In this study, the self-emulsification time for all developed formulations was measured using USP Apparatus II. The emulsification time for drug-loaded SNEDDS in experimental design batches was a key response in the optimization process, as summarized in Table 6. Ideally, self-emulsification should occur in less than 60 seconds to ensure rapid drug release and absorption. All experimental batches of NMD-SNEDDS achieved rapid emulsification, with time under 90 seconds, indicating that they can form emulsions spontaneously upon exposure to gastric fluid. The optimized NMD-SNEDDS formulation emulsified in 38.9 seconds, indicating a highly spontaneous system. No phase separation or drug precipitation was observed in any liquid SNEDDS formulations after 24 and 48 h of storage, confirming stability. The dilution of liquid SNEDDS did not affect the surfactant mixture's packing at the nanodroplet interface, and no precipitate formation occurred within 48 hours. Self-emulsification time is crucial for evaluating SNEDDS performance, affecting drug release and overall formulation effectiveness. The system must disperse completely and quickly in an aqueous phase under mild agitation, simulating conditions in the gastrointestinal tract [49].

Refractive index and percentage transmittance

The RI results for all experimental NMD-SNEDDS batches, as detailed in Table 6, showed RI values

Table 6 Characteristic parameters of developed formulations.

Batch Number	Emulsification time (s)	Refractive index	Percentage transparency(*T*%)	Zeta potential	Drug content
BBD1	85.2 ± 1.1	1.59 ± 0.02	98.59 ± 0.62	–12.70 ± 0.52	92.54% ± 0.20%
BBD2	36.0 ± 2.4	1.42 ± 0.03	100.42 ± 0.54	–16.48 ± 0.41	95.87% ± 0.64%
BBD3	75.4 ± 1.4	1.49 ± 0.05	99.49 ± 0.84	–17.85 ± 0.68	93.47% ± 0.52%
BBD4	80.4 ± 1.3	1.54 ± 0.02	100.54 ± 0.45	–18.01 ± 0.24	92.86% ± 0.41%
BBD5	32.1 ± 2.1	1.31 ± 0.04	99.31 ± 0.91	–13.68 ± 0.24	96.83% ± 0.12%
BBD6	30.0 ± 1.4	1.29 ± 0.06	98.29 ± 0.62	–14.75 ± 0.16	97.16% ± 0.64%
BBD7	36.1 ± 1.3	1.36 ± 0.07	100.36 ± 0.71	–17.85 ± 0.36	95.85% ± 0.65%
BBD8	39.0 ± 2.0	1.36 ± 0.02	99.36 ± 0.13	–13.59 ± 0.47	95.41% ± 0.41%
BBD9	33.1 ± 1.5	1.33 ± 0.03	98.33 ± 0.34	–14.23 ± 0.41	96.12% ± 0.51%
BBD10	30.1 ± 1.1	1.29 ± 0.01	100.29 ± 0.62	–15.98 ± 0.65	97.15% ± 0.69%
BBD11	78.4 ± 3.4	1.45 ± 0.08	100.45 ± 0.56	–14.32 ± 0.61	93.28% ± 0.54%
BBD12	35.5 ± 1.4	1.34 ± 0.04	99.34 ± 0.41	–17.42 ± 0.42	96.14% ± 0.65%
BBD13	32.4 ± 0.5	1.32 ± 0.05	99.54 ± 0.61	–16.24 ± 0.35	96.87% ± 0.45%
BBD14	30.2 ± 0.3	1.28 ± 0.03	100.10 ± 0.69	–18.12 ± 0.45	97.85% ± 0.84%
BBD15	39.4 ± 1.1	1.35 ± 0.04	99.54 ± 0.56	–17.85 ± 0.64	95.56% ± 0.24%

between 1.28 and 1.59, confirming their isotropic nature post-nanoemulsion transformation. The optimized batch had an RI of 1.37. Percentage transmittance (*T*%) studies further characterized the formulations, with all batches displaying nearly 100% transmittance, indicating high clarity. The optimized batch had a *T*% value of 99.48%. These results highlight the formulations' clarity and isotropic characteristics, essential for effective drug delivery. RI and *T*% are crucial for assessing the clarity, droplet size, and stability of SNEDDS formulations.

In vitro dissolution study

NMD is a hydrophobic drug with limited water solubility (log*p* = 3.5). *In-vitro* drug dissolution studies were conducted using hard gelatin capsules filled with optimized NMD-SNEDDS and NMD powder. The optimized NMD-SNEDDS exhibited a rapid dissolution rate, achieving nearly 90% release within 15 minutes across different media (pH 1.2, 6.8, and distilled water), highlighting its enhanced solubility [26]. In contrast, NMD powder displayed a slow release profile, with only 20% dissolution over 90 min. These findings underscore the need for improved oral delivery methods for NMD. Notably, the NMD-SNEDDS showed significantly superior dissolution enhancement ($p < 0.05$) in all media due to the efficient self-nanoemulsification process, which maintained the drug in a solubilized state within nano-sized oil droplets. The optimized formulation's enhanced dissolution rate and maximum percentage of release compared to NMD powder suggest that the SNEDDS's nano-sized particles provided a larger surface area, increasing dissolution. This improved dissolution rate is attributed to the reduced globule size, increased surface area, and decreased diffusion distance, leading to higher absorption and oral bioavailability of NMD.

Robustness to dilution

Ensuring the formation of uniform nanoemulsions during the self-emulsification of SNEDDS under various dilution conditions is crucial. The effects of dilution extent and the pH of the dilution medium on the optimized NMD-SNEDDS and MH-loaded NMD-SNEDDS were evaluated, with results summarized in Table 7. Regardless of pH or dilution volume, all systems maintained a globule size of approximately 130 nm. The optimized system demonstrated excellent robustness, with no phase separation or drug precipitation observed after 48 h of storage. This stability indicates that the oil phase, rather than the surfactant or co-surfactant, primarily contributes to drug solubilization. Robustness to dilution studies confirms the nanoemulsion's stability and suitability for oral use. For successful SNEDDS formulation, understanding factors affecting drug loading capacity is essential, ensuring that the system remains monophasic upon dilution with water or buffer, thus minimizing drug precipitation or crystallization.

Differential scanning calorimetry (DSC) analysis

The DSC analysis of pure NMD, pure MH, their physical mixture, NMD-SNEDDS, and MH-loaded NMD-SNEDDS are shown in Fig 7. The DSC thermogram of pure NMD revealed a sharp endothermic peak at 124 °C, indicative of its crystalline nature and corresponding closely to its melting point, confirming NMD's purity. Similarly, pure MH exhibited a broad endothermic peak at 290 °C, reflecting its crystallinity. In the physical mixture of NMD and MH, the NMD peak remained unchanged, indicating no chemical interaction between the two. However, in the NMD-SNEDDS and MH-loaded NMD-SNEDDS formulations, the absence of the NMD peak suggests a transition from crystalline to amorphous form. This transition indicates that NMD is molecularly dissolved within the SNEDDS, enhancing its solubility and dissolution rate [61].

Table 7 Globule size for optimized batches of NMD-SNEDDS with fraction of dilution (1:100).

Dilution media	Globule size (nm)	
	NMD-SNEDDS	MH-loaded NMD-SNEDDS
0.1 mol/L HCl	121.25 ± 1.11	131.25 ± 0.24
Water	123.14 ± 1.54	128.14 ± 1.43
Acetate buffer pH 4.5	123.17 ± 1.32	119.57 ± 1.73
Phosphate buffer pH 6.8	120.23 ± 0.98	119.72 ± 1.78
Phosphate buffer pH 7.4	123.10 ± 1.65	122.23 ± 1.98

Note: The results are given in mean ± SD ($n = 3$).

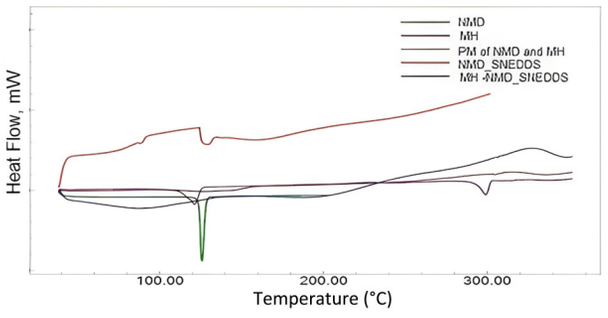

Fig. 7 Differential scanning calorimetric thermograms of NMD, MH, NMD and MH physical mixture, NMD-SNEDDS and MH-loaded NMD-SNEDDS.

FTIR spectroscopy analysis

The FTIR spectrum of pure NMD, MH, their physical mixture, optimized NMD-SNEDDS, and MH-loaded NMD-SNEDDS are shown in Fig. 8. The FTIR spectrum of NMD displayed a prominent band at 330 1.6 cm^{-1}, attributed to carboxylic functions. Signals at 2 981 and 2 932 cm^{-1} corresponded to C–H stretching in the aromatic ring and aliphatic chain. Other significant bands at 1 345, 3 088, 1 696, and 1 378 cm^{-1} were linked to the Nitro group, Pyridine, C=O, and CH_3 stretching, respectively. The physical

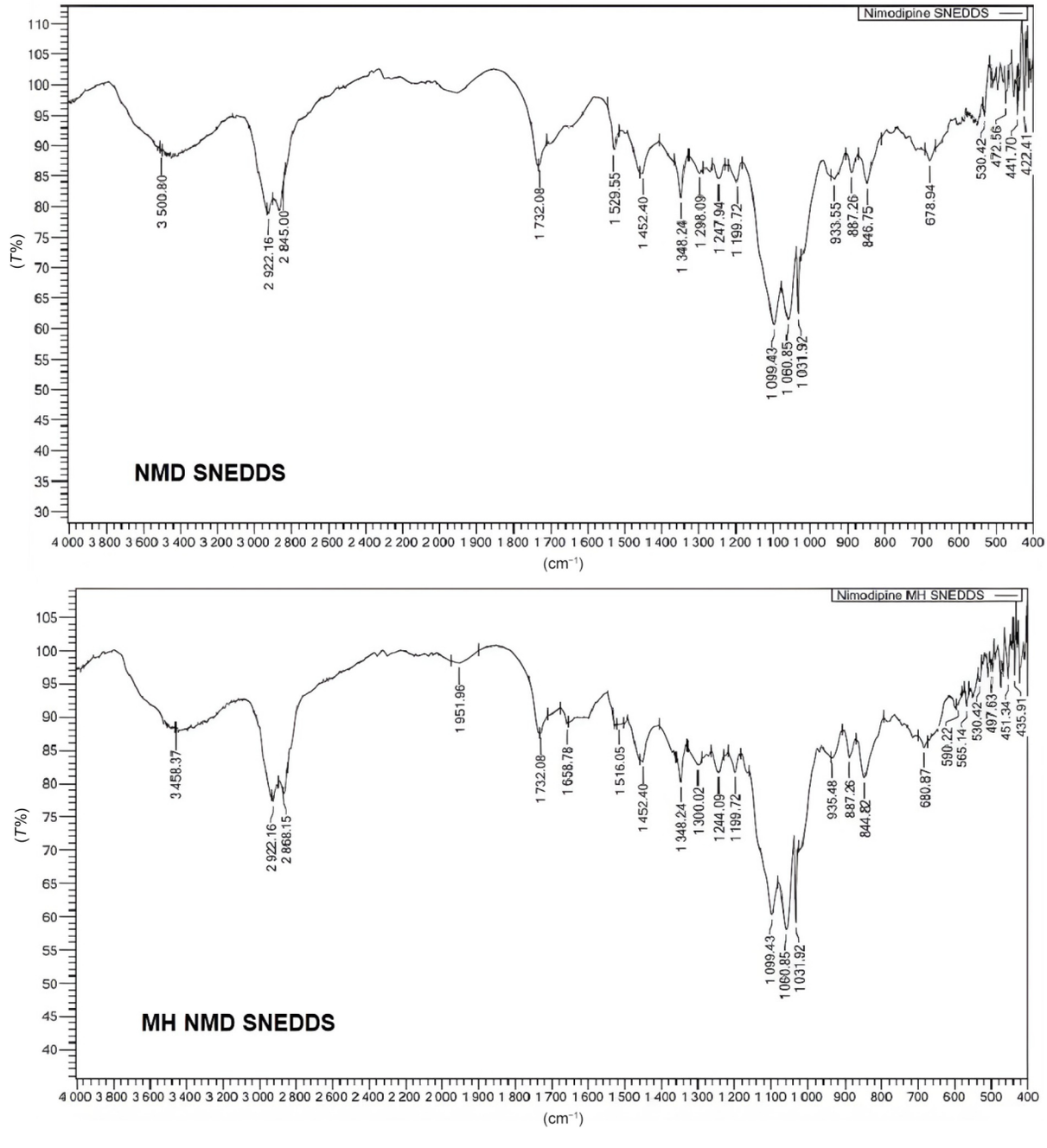

Fig. 8 FTIR spectrums of NMD-SNEDDS and MH-loaded NMD-SNEDDS.

mixture showed characteristic signals of both NMD and MH, indicating no chemical interaction. The NMD-SNEDDS and MH-loaded NMD-SNEDDS formulations retained all relevant absorption bands of NMD, confirming that NMD remained in its native form and was stable within the SNEDDS.

Transmission electron microscopy analysis

TEM is crucial for studying microstructures, providing high-resolution images that capture structural details and transitions [62]. The morphology and structure of MH-loaded NMD-SNEDDS formulations were examined using TEM, revealing discrete, spherical oil globules with diameters ranging from 125 to 155 nm. These globules appeared darker with bright surroundings. Figure 9 displays the droplet sizes of some dispersed oil globules measured by TEM, which closely align with the results obtained from Zetatrac analysis.

Cell viability

The MTT assay results demonstrated Caco-2 cell viability following exposure to the Control, NMD, NMD-SNEDDS, and MH-loaded NMD-SNEDDS, as illustrated in Fig. 10. All three formulations (NMD, NMD-SNEDDS, and MH-loaded NMD-SNEDDS) were non-toxic at concentrations up to 0.1% (v/v). However, at higher concentrations, the toxicity levels varied between the groups (Fig. 10). The toxicity ranking in Caco-2 cells was NMD > NMD-SNEDDS ≈ MH-loaded NMD-SNEDDS. There was no significant difference in toxicity between NMD-SNEDDS and MH-loaded NMD-SNEDDS. Given that the toxicity values of NMD-SNEDDS and MH-loaded NMD-SNEDDS were nearly identical to NMD, the nanoemulsion formulation and MH loading did not increase toxicity in Caco-2 cells. These findings suggest that administering MH-loaded NMD-SNEDDS orally at the same NMD dose for antihypertensive purposes would not result in increased cellular toxicity.

In vivo pharmacokinetic studies

The pharmacokinetic behavior of NMD was investigated following oral administration of optimized NMD-SNEDDS, MH-loaded NMD-SNEDDS, a marketed NMD formulation, and pure NMD suspension in rats. The plasma concentration profiles (Fig. 11) revealed that NMD levels were consistently higher in both NMD-SNEDDS and MH-loaded NMD-SNEDDS compared to the marketed formulation and pure drug. This increased bioavailability is attributed to the rapid dissolution of NMD from SNEDDS, as shown by nearly 90% drug release within 15 min. The plasma concentration evolution trend in Fig. 11 reflects a complex pharmacokinetic profile rather than a simple decay function. The observed plateaus in the curve may

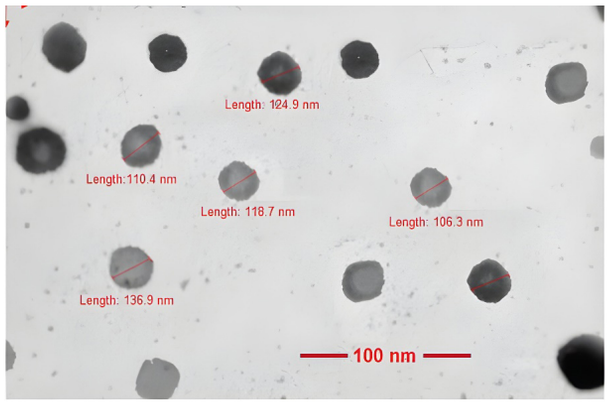

Fig. 9 TEM image of MH-loaded NMD-SNEDDS.

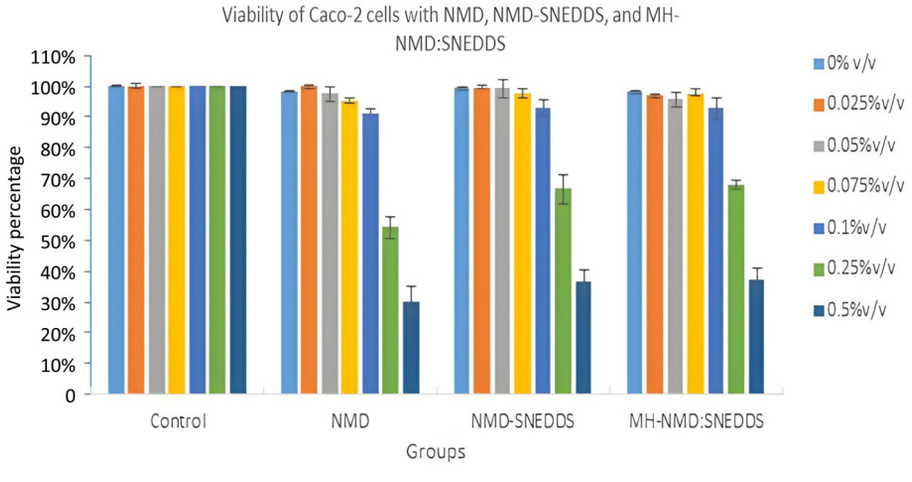

Fig. 10 Viability of Caco-2 cells with NMD, NMD-SNEDDS, and MH-loaded NMD-SNEDDS.

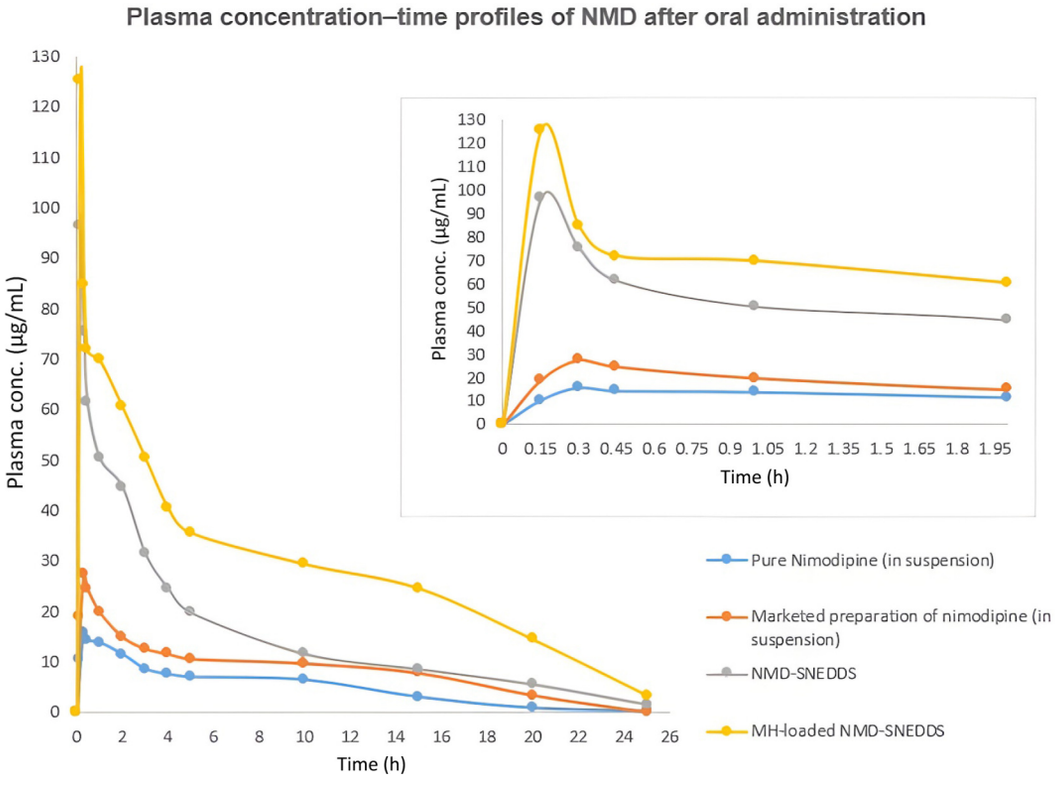

Fig. 11 Plasma concentration profiles of NMD after oral administration of pure NMD, marketed preparation, NMD-SNEDDS and MH-loaded NMD-SNEDDS.

indicate phases of sustained release or absorption, which can occur due to factors such as the formulation's release characteristics or interactions between the drug and biological components. Additionally, these plateaus might result from the drug's distribution dynamics or it's binding to plasma proteins, leading to temporary stabilization of the plasma concentration before subsequent elimination. Pharmacokinetic analysis (Table 8) indicated that NMD-SNEDDS exhibited 6- and 3-fold higher C_{max} and AUC values, respectively, while MH-loaded NMD-SNEDDS showed 8- and 4-fold increases in C_{max} and AUC values compared to pure NMD. The inclusion of MH in SNEDDS significantly enhanced the oral bioavailability of NMD compared to SNEDDS without MH. Notably, MH-containing SNEDDS increased drug retention in the body, as evidenced by reduced drug clearance (1.47 ± 0.42 L/h) compared to NMD-SNEDDS or suspension. This improvement is likely due to MH facilitating transcellular absorption without disrupting tight junctions, as confirmed by cellular uptake studies. The reduced T_{max} indicates rapid intraluminal emulsification into nano-sized droplets, enhancing surface area and drug absorption. These findings suggest that both SNEDDS formulations offer a promising strategy for rapid absorption and improved bioavailability of poorly water-soluble drugs like NMD. The primary mechanism behind the increased bioavailability of SNEDDS is the spontaneous

Table 8 Pharmacokinetic parameters of NMD after the Oral administration of an optimized NMD-SNEDDS, MH-loaded NMD-SNEDDS, marketed preparation of nimodipine and pure nimodipine.

Parameters	Pure NMD (in suspension)	Marketed preparation of NMD (in suspension)	NMD-SNEDDS	MH-loaded NMD-SNEDDS
C_{max} (μg/mL)	15.82 ± 2.06	27.45 ± 3.17	96.45 ± 3.17	125.36 ± 5.34
T_{max} (h)	0.31 ± 0.12	0.28 ± 0.35	0.15 ± 0.35	0.14 ± 0.29
$t_{1/2}$ (h)	2.50 ± 0.40	2.10 ± 0.14	1.30 ± 0.34	1.29 ± 1.14
AUC_{0-24} (h·μg/mL)	86.54 ± 15.46	103.54 ± 18.25	288.32 ± 23.13	376.16 ± 28.51
$AUC_{0-\infty}$ (h·μg/mL)	93.21 ± 20.12	110.54 ± 18.27	297.54 ± 26.51	386.31 ± 35.14
Clearance (L/h)	4.84 ± 0.19	3.95 ± 0.24	1.91 ± 0.28	1.47 ± 0.42

nanoemulsification in gastrointestinal fluid, presenting the drug in a solubilized form with smaller droplet sizes and greater interfacial area [42, 57]. This improves drug solubilization in the GI lumen, enhancing bioavailability. Additional mechanisms include surfactant-mediated permeability enhancement through the disruption of tight junctions, increased lymphatic transport, and reduced hepatic first-pass metabolism due to the lipid content in the formulation. The research conducted on other antihypertensive drug by Mekala S. [63] indicate that enalapril maleate encapsulated within nanoproniosomal gels can effectively function as controlled drug delivery systems, releasing the drug once per day for effective hypertension management.

Study of P-gp inhibition activity

Verapamil, a widely studied cardiovascular drug and P-gp substrate, is ideal for investigating P-gp inhibition activity. The IC_{10} values of NMD-SNEDDS and MH-loaded NMD-SNEDDS were 10 and 7.5 μg/mL, respectively, compared to Verapamil's IC_{50} value of 185.20 μg/mL. Co-treatment with these formulations and Verapamil reduced the IC_{50} of Verapamil to 164.54 μg/mL for NMD-SNEDDS and 131.39 μg/mL for MH-loaded NMD-SNEDDS, indicating enhanced inhibition. Cremophor RH-40, present in the formulations, is known to enhance bioavailability by inhibiting P-gp and CYP450 enzymes, thus reducing intestinal efflux and promoting drug absorption. Morin hydrate (MH) further inhibits P-gp and CYP3A4, leading to increased drug absorption. The enhanced C_{max} and AUC values are due to improved solubility and dissolution rates, which increase membrane fluidity and facilitate diffusion across biological membranes. MH-loaded NMD-SNEDDS showed higher bioavailability than NMD-SNEDDS alone, addressing NMD's reduced oral bioavailability caused by both CYP3A4 metabolism and P-glycoprotein efflux [64]. SNEDDS components, such as surfactants and oils, act as P-glycoprotein inhibitors and absorption enhancers, improving the oral bioavailability of their loaded drugs. The smaller droplet size of SNEDDS also contributes to this enhancement. Morin modulates metabolic enzymes and P-glycoprotein efflux, as reported by Choi et al. [65], who found that co- and pre-administration of morin significantly increased the Cmax and AUC of drugs like nimodipine and diltiazem, both P-glycoprotein and CYP3A4 substrates. In current research work, morin act as a dual inhibitor of CYP3A4 and P-glycoprotein. This inhibition reduces NMD efflux, leading to improved absorption and higher bioavailability, especially in MH-loaded NMD-SNEDDS.

Stability study

Stability studies for the optimized NMD-SNEDDS and MH-loaded NMD-SNEDDS formulations were conducted according to ICH guidelines at (40 ± 2) °C/(75±5) RH% over six months. The formulations exhibited good stability, with no significant changes in physical or chemical properties. As shown in Table 9, there were no marked differences between the initial and aged samples after six months. Shelf life (t_{90}) was estimated by extrapolating the drug assay data over time, with the lower 95% confidence limit intersecting the acceptance criteria at 18 months for NMD-SNEDDS and 15 months for MH-loaded NMD-SNEDDS.

Conclusions

NMD is widely used for treating subarachnoid hemorrhage (SAH) but suffers from low and variable oral bioavailability due to poor solubility and extensive first-pass metabolism by CYP enzymes, especially CYP 3A4. To address these issues, a

Table 9 Results of Accelerated Stability Study for NMD-SNEDDS and MH-Loaded NMD-SNEDDS.

Parameters	Storage Period					
	NMD-SNEDDS			MH-loaded NMD-SNEDDS		
	0	3 months	6 months	0	3 months	6 months
Assay	94.9% ± 0.3%	94.1% ± 0.6%	91.8% ± 0.5%	92.5% ± 0.2%	92.1%± 0.5%	90.5% ± 0.7%
Globule size (nm)	130.4 ± 0.9	137.6 ± 0.4	142.4 ± 0.6	138.2 ± 0.7	141.2 ± 0.8	145.2 ± 0.3
PDI	0.102 ± 0.012	0.110 ± 0.021	0.114 ± 0.008	0.112 ± 0.012	0.110 ± 0.012	0.118 ± 0.023
Zeta potential (mV)	–19.12 ± 0.54	–17.65 ± 0.41	–17.12 ± 0.22	–18.41 ± 0.23	–17.62 ± 0.41	–16.35 ± 0.41

Note: The results are given in mean ± SD (n = 3).

SNEDDS formulation containing morin hydrate was developed. This formulation included 10.0 mg of nimodipine, 62.0 mg of Capmul MCM as the oil, 40.0 mg of Cremophor RH-40 as the surfactant, and Transcutol-P as the co-surfactant to improve nimodipine's oral bioavailability. A BBD was used to assess the interaction and quadratic effects of these variables. Optimization with a desirability function resulted in a formulation where observed responses closely matched predicted values. Both *in vitro* dissolution studies and *in vivo* pharmacokinetic studies showed that the NMD-SNEDDS formulation provided faster drug dissolution and higher bioavailability compared to NMD powder and marketed formulations. The system demonstrated stability against temperature, dilution, and pH changes, with no toxicity and effective membrane permeation. While promising, extensive clinical trials are needed before commercialization.

Ethics Approval and Consent to Participate

All experimental procedures were conducted in accordance with the principles outlined for the use of animals in toxicology, as recommended by the Institutional Animal Ethics Committee (IAEC), CPCSEA, Government of India. The study was approved by IAEC (Protocol number: IAEC/DPS/SU/1511).

CRediT Author Statement

Nirav Patel: conceptualization, methodology, supervision, and original draft preparation. **Dhara Thummar:** formal analysis, investigation, and resources. **Priya Patel:** data curation, writing–reviewing, and editing.

Acknowledgements

The authors express their sincere gratitude to the Head and Faculties of the Department of Pharmaceutical Sciences, Saurashtra University, Rajkot, India, for generously providing the research facilities and necessary support essential for conducting this study. Their support and assistance throughout the duration of the research are greatly appreciated.

Conflict of Interests

The authors declare no conflict of interest, financial or otherwise.

References

[1] S. Thilak, P. Brown, T. Whitehouse, et al. Diagnosis and management of subarachnoid haemorrhage. *Nature Communications*, 2024, 15: 1850. https://doi.org/10.1038/s41467-024-46015-2

[2] N. Etminan, H.S. Chang, K. Hackenberg, et al. Worldwide incidence of aneurysmal subarachnoid hemorrhage according to region, time period, blood pressure, and smoking prevalence in the population. *JAMA Neurology*, 2019, 76(5): 588. https://doi.org/10.1001/jamaneurol.2019.0006

[3] F. Ikawa, N. Michihata, T. Matsushige, et al. In-hospital mortality and poor outcome after surgical clipping and endovascular coiling for aneurysmal subarachnoid hemorrhage using nationwide databases: A systematic review and meta-analysis. *Neurosurgical Review*, 2020, 43(2): 655−667. https://doi.org/10.1007/s10143-019-01096-2

[4] G.S. Allen, H.S. Ahn, T.J. Preziosi, et al. Cerebral arterial spasm–A controlled trial of nimodipine in patients with subarachnoid hemorrhage. *New England Journal of Medicine*, 1983, 308(11): 619−624. https://doi.org/10.1056/nejm198303173081103

[5] J.D. Pickard, G.D. Murray, R. Illingworth, et al. Effect of oral nimodipine on cerebral infarction and outcome after subarachnoid haemorrhage: British aneurysm nimodipine trial. *Bmj*, 1989, 298(6674): 636−642. https://doi.org/10.1136/bmj.298.6674.636

[6] Y.F. Liu, H.C. Qiu, J. Su, et al. Drug treatment of cerebral vasospasm after subarachnoid hemorrhage following aneurysms. *Chinese Neurosurgical Journal*, 2016, 2(1): 4. https://doi.org/10.1186/s41016-016-0023-x

[7] Z.J. Teng, M. Yu, Y. Ding, et al. Preparation and characterization of nimodipine-loaded nanostructured lipid systems for enhanced solubility and bioavailability. *International Journal of Nanomedicine*, 2018, 14: 119−133. https://doi.org/10.2147/ijn.s186899

[8] S.H. Mahmoud, X.Q. Ji, F.A. Isse. Nimodipine pharmacokinetic variability in various patient populations. *Drugs in R&D*, 2020, 20(4): 307−318. https://doi.org/10.1007/s40268-020-00322-3

[9] L. Zhang, X.D. Liu, L. Xie, et al. P-glycoprotein restricted transport of nimodipine across blood-brain barrier. *Acta Pharmacologica Sinica*, 2003, 24(9): 903−906.

[10] A. Elizabeth, A. Adegbuyi, A. Olusegun, et al. Morin hydrate attenuates chronic stress-induced memory impairment and degeneration of hippocampal subfields in mice: The role of oxidative, nitrergic and neuroinflammatory pathways. *Metabolic Brain Disease*, 2020, 35(7): 1145−1156. https://doi.org/10.1007/s11011-020-00595-2

[11] M. Kumar, U. Kumar, A.K. Singh. Therapeutic nanoparticles: Recent developments and their targeted delivery applications. *Nano Biomedicine and Engineering*, 2022, 14(1): 38−52. https://doi.org/10.5101/nbe.v14i1.p38-52

[12] J.S. Choi, J.P. Burm. Enhanced nimodipine bioavailability after oral administration of nimodipine with morin, a flavonoid, in rabbits. *Archives of Pharmacal Research*, 2006, 29(4): 333−338. https://doi.org/10.1007/BF02968580

[13] D.V. Bhalani, B. Nutan, A. Kumar, et al. Bioavailability enhancement techniques for poorly aqueous soluble drugs and therapeutics. *Biomedicines*, 2022, 10(9): 2055. https://

doi.org/10.3390/biomedicines10092055
[14] A.B. Buya, A. Beloqui, P.B. Memvanga, et al. Self-nano-emulsifying drug-delivery systems: From the development to the current applications and challenges in oral drug delivery. *Pharmaceutics*, 2020, 12(12): 1194. https://doi.org/10.3390/pharmaceutics12121194
[15] T.H. Huang, C.J. Chen, H.C.A. Lin, et al. Self-nanoemulsifying drug delivery system-containing the poorly absorbed drug–valsartan in post-bariatric surgery. *International Journal of Nanomedicine*, 2023, 18: 2647−2658. https://doi.org/10.2147/ijn.s394624
[16] I.K. Abbas. Self-nanoemulsifying drug delivery system: Liquid, supersaturable, and solid dosage forms. *Al-Rafidain Journal of Medical Sciences*, 2022, 3: 98−108. https://doi.org/10.54133/ajms.v3i.91
[17] S. Bandyopadhyay, S. Beg, O. Katare, et al. QbD-oriented development of self-nanoemulsifying drug delivery systems (SNEDDS) of valsartan with improved biopharmaceutical performance. *Current Drug Delivery*, 2015, 12(5): 544−563. https://doi.org/10.2174/1567201812666150227125639
[18] S.S. Buddhadev, K.C. Garala, S. Saisivam, et al. Quality by design aided self-nano emulsifying drug delivery systems development for the oral delivery of benidipine: Improvement of biopharmaceutical performance. *Drug Delivery*, 2024, 31(1): 2288801. https://doi.org/10.1080/10717544.2023.2288801
[19] K.C. Panigrahi, J. Jena, G.K. Jena, et al. QBD-based systematic development of bosentan SNEDDS: Formulation, characterization and pharmacokinetic assessment. *Journal of Drug Delivery Science and Technology*, 2018, 47: 31−42. https://doi.org/10.1016/j.jddst.2018.06.021
[20] G. Kuruba, K.A. Narayana Reddy, S. Poli, et al. Quality by design based development of self nano emulsifying drug delivery system of ritonavir. *Journal of Young Pharmacists*, 2020, 12(3): 215−220. https://doi.org/10.5530/jyp.2020.12.63
[21] P. Yadav, V. Rastogi, A. Verma. Application of Box–Behnken design and desirability function in the development and optimization of self-nanoemulsifying drug delivery system for enhanced dissolution of ezetimibe. *Future Journal of Pharmaceutical Sciences*, 2020, 6: 7. https://doi.org/10.1186/s43094-020-00023-3
[22] D.Y. Usta, B. Timur, Z.S. Teksin. Formulation development, optimization by box-behnken design, characterization, *in vitro, ex-vivo*, and *in vivo* evaluation of bosentan-loaded self-nanoemulsifying drug delivery system: A novel alternative dosage form for pulmonary arterial hypertension treatment. *European Journal of Pharmaceutical Sciences*, 2022, 174: 106159. https://doi.org/10.1016/j.ejps.2022.106159
[23] N. Marasini, Y.D. Yan, B.K. Poudel, et al. Development and optimization of self-nanoemulsifying drug delivery system with enhanced bioavailability by Box–Behnken design and desirability function. *Journal of Pharmaceutical Sciences*, 2012, 101(12): 4584−4596. https://doi.org/10.1002/jps.23333
[24] S. Khoshyari, R. Mahjub. Preparation, Box-Behnken statistical optimization, and *in vitro* characterization of a self-nanoemulsifying drug delivery system for the oral delivery of budesonide as a poorly soluble drug. *Avicenna Journal of Pharmaceutical Research*, 2020, 1(1): 24−32. https://doi.org/10.34172/ajpr.2020.05
[25] S.S. Chalikwar, V.S. Belgamwar, V.R. Talele, et al. Formulation and evaluation of Nimodipine-loaded solid lipid nanoparticles delivered *via* lymphatic transport system. *Colloids and Surfaces B: Biointerfaces*, 2012, 97: 109−116. https://doi.org/10.1016/j.colsurfb.2012.04.027
[26] D.B. Yang, J.B. Zhu, Y. Zheng, et al. Preparation, characterization, and pharmacokinetics of sterically stabilized nimodipine-containing liposomes. *Drug Development and Industrial Pharmacy*, 2006, 32(2): 219−227. https://doi.org/10.1080/03639040500466270
[27] D.F. do Nascimento, M.O. de Moraes, F.A.F. Bezerra, et al. Determination of nimodipine in plasma by HPLC-MS/MS and pharmacokinetic application. *Brazilian Journal of Pharmaceutical Sciences*, 2010, 46(4): 665−677. https://doi.org/10.1590/s1984-82502010000400008
[28] B. Rajani, K. Mukkanti. Optimized and validated RP-HPLC method for the estimation of nimodipine in tablet dosage form. *International Journal of Research in Pharmacy and Chemistry*, 2014, 4(1): 105–109.
[29] S. Akula, A.K. Gurram, S.R. Devireddy, et al. Evaluation of surfactant effect on self micro emulsifying drug delivery system (SMEDDS) of lercanidipine hydrochloride: Formulation and evaluation. *Journal of Pharmaceutical Innovation*, 2015, 10(4): 374−387. https://doi.org/10.1007/s12247-015-9233-6
[30] A.K. Singh, A. Chaurasiya, M. Singh, et al. Exemestane loaded self-microemulsifying drug delivery system (SMEDDS): Development and optimization. *AAPS PharmSciTech*, 2008, 9(2): 628−634. https://doi.org/10.1208/s12249-008-9080-6
[31] E. Abdelhakeem, M.H. Teaima, G.A. Abdelbary, et al. Bioavailability enhanced clopidogrel-loaded solid SNEDDS: Development and *in-vitro*/*in-vivo* characterization. *Journal of Drug Delivery Science and Technology*, 2019, 49: 603−614. https://doi.org/10.1016/j.jddst.2018.12.027
[32] J. Patel, A. Dhingani, K. Garala, et al. Quality by design approach for oral bioavailability enhancement of Irbesartan by self-nanoemulsifying tablets. *Drug Delivery*, 2014, 21(6): 412−435. https://doi.org/10.3109/10717544.2013.853709
[33] A. Azeem, M. Rizwan, F. Ahmad, et al. Components screening and influence of surfactant and cosurfactant on nanoemulsion formation. *Current Nanoscience*, 2009, 5(2): 220−226. https://doi.org/10.2174/157341309788185505
[34] D.Q.M. Craig, S.A. Barker, D. Banning, et al. An investigation into the mechanisms of self-emulsification using particle size analysis and low frequency dielectric spectroscopy. *International Journal of Pharmaceutics*, 1995, 114(1): 103−110. https://doi.org/10.1016/0378-5173(94)00222-q
[35] Z.C. Ke, X.F. Hou, X.B. Jia. Design and optimization of self-nanoemulsifying drug delivery systems for improved bioavailability of cyclovirobuxine D. *Drug Design, Development and Therapy*, 2016, 10: 2049−2060. https://doi.org/10.2147/dddt.s106356
[36] Z.Y. Wang, J. Sun, Y.J. Wang, et al. Solid self-emulsifying nitrendipine pellets: Preparation and *in vitro*/*in vivo* evaluation. *International Journal of Pharmaceutics*, 2010, 383(1-2): 1−6. https://doi.org/10.1016/j.ijpharm.2009.08.014
[37] S. Beg, O.P. Katare, S. Saini, et al. Solid self-nanoemulsifying systems of olmesartan medoxomil: Formulation development, micromeritic characterization, *in vitro* and *in vivo* evaluation. *Powder Technology*, 2016, 294: 93−104. https://doi.org/10.1016/j.powtec.2016.02.023
[38] G. Derringer, R. Suich. Simultaneous optimization of several response variables. *Journal of Quality Technology*, 1980, 12(4): 214−219. https://doi.org/10.1080/00224065.1980.11980968
[39] K.J. Kim, D.K.J. Lin. Simultaneous optimization of mechanical properties of steel by maximizing exponential desirability functions. *Journal of the Royal Statistical Society Series C: Applied Statistics*, 2000, 49(3): 311−325. https://doi.org/10.1111/1467-9876.00194
[40] H.J. Cho, D.W. Lee, N. Marasini, et al. Optimization of self-microemulsifying drug delivery system for telmisartan using Box–Behnken design and desirability function. *Journal of Pharmacy and Pharmacology*, 2013, 65(10): 1440−1450. https://doi.org/10.1111/jphp.12115
[41] Y. Liu, P. Zhang, N.P. Feng, et al. Optimization and *in situ* intestinal absorption of self-microemulsifying drug delivery system of oridonin. *International Journal of*

Pharmaceutics, 2009, 365(1-2): 136−142. https://doi.org/10.1016/j.ijpharm.2008.08.009
[42] R. Gannu, C.R. Palem, V.V. Yamsani, et al. Enhanced bioavailability of lacidipine via microemulsion based transdermal gels: Formulation optimization, *ex vivo* and *in vivo* characterization. *International Journal of Pharmaceutics*, 2010, 388(1-2): 231−241. https://doi.org/10.1016/j.ijpharm.2009.12.050
[43] T. Kanwal, M. Kawish, R. Maharjan, et al. Design and development of permeation enhancer containing self-nanoemulsifying drug delivery system (SNEDDS) for ceftriaxone sodium improved oral pharmacokinetics. *Journal of Molecular Liquids*, 2019, 289: 111098. https://doi.org/10.1016/j.molliq.2019.111098
[44] M.A. Altamimi, M. Kazi, M. Hadi Albgomi, et al. Development and optimization of self-nanoemulsifying drug delivery systems (SNEDDS) for curcumin transdermal delivery: An anti-inflammatory exposure. *Drug Development and Industrial Pharmacy*, 2019, 45(7): 1073−1078. https://doi.org/10.1080/03639045.2019.1593440
[45] Y.S.R. Elnaggar, M.A. El-Massik, O.Y. Abdallah. Self-nanoemulsifying drug delivery systems of tamoxifen citrate: Design and optimization. *International Journal of Pharmaceutics*, 2009, 380(1-2): 133−141. https://doi.org/10.1016/j.ijpharm.2009.07.015
[46] L. Mandpe, V. Pokharkar. Quality by design approach to understand the process of optimization of iloperidone nanostructured lipid carriers for oral bioavailability enhancement. *Pharmaceutical Development and Technology*, 2015, 20(3): 320−329. https://doi.org/10.3109/10837450.2013.867445
[47] E.A. Mahmoud, E.R. Bendas, M.I. Mohamed. Preparation and evaluation of self-nanoemulsifying tablets of carvedilol. *AAPS PharmSciTech*, 2009, 10(1): 183−192. https://doi.org/10.1208/s12249-009-9192-7
[48] A.B. Buya, B. Ucakar, A. Beloqui, et al. Design and evaluation of self-nanoemulsifying drug delivery systems (SNEDDSs) for senicapoc. *International Journal of Pharmaceutics*, 2020, 580: 119180. https://doi.org/10.1016/j.ijpharm.2020.119180
[49] L.Y. Zeng, Y.L. Zhang. Development, optimization and *in vitro* evaluation of norcantharidin loadedself-nanoemulsifying drug delivery systems (NCTD-SNEDDS). *Pharmaceutical Development and Technology*, 2017, 22(3): 399−408. https://doi.org/10.1080/10837450.2016.1219915
[50] K.F. Alhasani, M. Kazi, M. Abbas, et al. Self-nanoemulsifying ramipril tablets: A novel delivery system for the enhancement of drug dissolution and stability. *International Journal of Nanomedicine*, 2019, 14: 5435−5448. https://doi.org/10.2147/ijn.s203311
[51] B. Morakul, V. Teeranachaideekul, W. Limwikrant, et al. Dissolution and antioxidant potential of apigenin self nanoemulsifying drug delivery system (SNEDDS) for oral delivery. *Scientific Reports*, 2024, 14: 8851. https://doi.org/10.1038/s41598-024-59617-z
[52] M. Kazi, M. Al-Swairi, A. Ahmad, et al. Evaluation of self-nanoemulsifying drug delivery systems (SNEDDS) for poorly water-soluble talinolol: Preparation, *in vitro* and *in vivo* assessment. *Frontiers in Pharmacology*, 2019, 10: 459. https://doi.org/10.3389/fphar.2019.00459
[53] D. Zaafar, H.M.A. Khalil, G.E. Elkhouly, et al. Preparation and characterization of sorafenib nano-emulsion: impact on pharmacokinetics and toxicity; an in vitro and in vivo study. *Drug Delivery and Translational Research*, 2024, 14(11): 3089−3111. https://doi.org/10.1007/s13346-024-01530-z
[54] L.Y. Kok, P. Bannigan, F. Sanaee, et al. Development and pharmacokinetic evaluation of a self-nanoemulsifying drug delivery system for the oral delivery of cannabidiol. *European Journal of Pharmaceutical Sciences*, 2022, 168: 106058. https://doi.org/10.1016/j.ejps.2021.106058
[55] T.T.L. Nguyen, V.A. Duong, H.J. Maeng. Pharmaceutical formulations with P-glycoprotein inhibitory effect as promising approaches for enhancing oral drug absorption and bioavailability. *Pharmaceutics*, 2021, 13(7): 1103. https://doi.org/10.3390/pharmaceutics13071103
[56] C. Rathore, C. Hemrajani, A.K. Sharma, et al. Self-nanoemulsifying drug delivery system (SNEDDS) mediated improved oral bioavailability of thymoquinone: Optimization, characterization, pharmacokinetic, and hepatotoxicity studies. *Drug Delivery and Translational Research*, 2023, 13(1): 292−307. https://doi.org/10.1007/s13346-022-01193-8
[57] K. Bunchongprasert, J. Shao. Cytotoxicity and permeability enhancement of Capmul®MCM in nanoemulsion formulation. *International Journal of Pharmaceutics*, 2019, 561: 289−295. https://doi.org/10.1016/j.ijpharm.2019.03.010
[58] H.N. Prajapati, D.P. Patel, N.G. Patel, et al. Effect of difference in fatty acid chain lengths of medium-chain lipids on lipid/surfactant/water phase diagrams and drug solubility. *Journal of Excipients and Food Chemicals*, 2011, 2(3): 73−88.
[59] M. Kong, H.J. Park. Stability investigation of hyaluronic acid based nanoemulsion and its potential as transdermal carrier. *Carbohydrate Polymers*, 2011, 83(3): 1303−1310. https://doi.org/10.1016/j.carbpol.2010.09.041
[60] M. Kazi, A. Alhajri, S.M. Alshehri, et al. Enhancing oral bioavailability of apigenin using a bioactive self-nanoemulsifying drug delivery system (Bio-SNEDDS): In vitro, in vivo, and stability evaluations. *Pharmaceutics*, 2020, 12(8): 749. https://doi.org/10.3390/pharmaceutics12080749
[61] Y. Zhao, T.G. Xin, T.T. Ye, et al. Solid dispersion in the development of a nimodipine delayed-release tablet formulation. *Asian Journal of Pharmaceutical Sciences*, 2014, 9(1): 35−41. https://doi.org/10.1016/j.ajps.2013.11.006
[62] M.N. Mohd Izham, Y. Hussin, M.N.M. Aziz, et al. Preparation and characterization of self nano-emulsifying drug delivery system loaded with citraland its antiproliferative effect on colorectal cells *in vitro*. *Nanomaterials*, 2019, 9(7): 1028. https://doi.org/10.3390/nano9071028
[63] M. Sabareesh, J. Rajangam, J.P. Yanadaiah. Formulation of enalapril maleate nanoproniosomal gels and their pharmacokinetic evaluations in hypertensive albino wistar rats: *Ex vivo* and *in vivo* approaches. *Nano Biomedicine and Engineering*, 2024, 16(3): 429−442. https://doi.org/10.26599/nbe.2024.9290084
[64] H. Nguyen, S.Z. Zhang, M.E. Morris. Effect of flavonoids on MRP1-mediated transport in Panc-1 cells. *Journal of Pharmaceutical Sciences*, 2003, 92(2): 250−257. https://doi.org/10.1002/jps.10283
[65] J.S. Choi, H.K. Han. Pharmacokinetic interaction between diltiazem and morin, a flavonoid, in rats. *Pharmacological Research*, 2005, 52(5): 386−391. https://doi.org/10.1016/j.phrs.2005.05.011